Advances in Nano Research, *Vol. 15, No. 4 (2023) 367-384*
https://doi.org/10.12989/anr.2023.15.4.367

Natural frequency analysis of joined conical-cylindrical-conical shells made of graphene platelet reinforced composite resting on Winkler elastic foundation

Xiangling Wang**[1], Xiaofeng Guo[2], Masoud Babaei*[3], Rasoul Fili[4] and Hossein Farahani[5]

[1]*Department of Mining Engineering, Lyuliang University, Luliang, China*
[2]*College of information Science and Engineering, Shanxi Agricultural University, Taigu, China*
[3]*Department of Mechanical Engineering, University of Eyvanekey, Eyvanekey, Semnan, Iran*
[4]*Department of Engineering, Imam Ali University, Tehran, Iran*
[5]*Department of Civil engineering, Islamic Azad University,Central Tehran Branch, Tehran, Iran*

(*Received February 8, 2022, Revised April 7, 2023, Accepted May 2, 2023*)

Abstract. Natural frequency behavior of graphene platelets reinforced composite (GPL-RC) joined truncated conical–cylindrical- conical shells resting on Winkler-type elastic foundation is presented in this paper for the first time. The rule of mixture and the modified Halpin-Tsai approach are applied to achieve the mechanical properties of the structure. Four different graphene platelets patterns are considered along the thickness of the structure such as GPLA, GPLO, GPLX, GPLUD. Finite element procedure according to Rayleigh-Ritz formulation has been used to solve 2D-axisymmetric elasticity equations. Application of 2D axisymmetric elasticity theory allows thickness stretching unlike simple shell theories, and this gives more accurate results, especially for thick shells. An efficient parametric investigation is also presented to show the effects of various geometric variables, three different boundary conditions, stiffness of elastic foundation, dispersion pattern and weight fraction of GPLs nanofillers on the natural frequencies of the joined shell. Results show that GPLO and BC3 provide the most rigidity that cause the most natural frequencies among different BCs and GPL patterns. Also, by increasing the weigh fraction of nanofillers, the natural frequencies will increase up to 200%.

Keywords: finite element method; graphene platelets-reinforced composites; joined truncated conical-cylindrical-conical shell; natural frequency analysis; Winkler elastic foundation

1. Introduction

Cylindrical and conical shell structures have been used in various industries and engineering applicants. However, joined shells comprising different cylindrical, conical and spherical shell sections are employed specially in submarine structures and aerospace engineering. These types of structures are mostly under aerodynamic forces. Therefore, it is of significance and value to prevent the resonance phenomenon in these structures with sensitive applications in engineering. Revolution of the problem of natural frequencies of shell structures with different kinds of geometries including spherical, cylindrical and conical shell structures has been the title of different works so far. Therefore, the subject is presented in numerous textbooks and investigations, see for instance, (Leissa 1993, Qatu 2004, Soedel 2004, Ebrahimi and Seyfi 2020, Jrad *et al*. 2019; Babaei and Asemi 2020a, Babaei and Asemi 2020b). However, the natural frequency characteristics of joined shell structures are limited because the most number of resulting equations and complexity which may appear while using the continuity and boundary conditions. For example, Irie *et al*. (1984) investigated free vibration of joined conical-cylindrical shells using first order shear deformation theory (FSDT) and applying the transfer matrix of the structure. Lee *et al*. (2002) investigated natural frequencies of the joined cylindrical–spherical shell structures with various end conditions applying Rayleigh's energy procedure and Flügge shell theory. Shakouri and Kouchakzadeh (2014) carried out an investigation about natural frequency analysis of joined conical shells analytically and experimentally. The governing equation was obtained applying Hamilton′s principle and Donnell shell theory. Applying Reissner-Naghdi's thin shell theory, a variational approach for natural frequency analysis of joined conical- cylindrical shells was presented by Qu *et al*. (2013). Patel, Ganapathi, and Kamat (2000) analyzed natural frequency characteristics of laminated composite joined cylindrical-conical shells by applying finite element method (FEM). Bagheri *et al*. (2018) examined natural frequency of isotropic homogeneous joined conical–cylindrical–conical shells according to FSDT and employing generalized differential quadrature (GDQ) procedure. In another research, based on FSDT and employing GDQ method, Bagheri *et al*. (2020) studied natural frequency of joined cylindrical–hemispherical shells made of functionally graded materials (FGMs). Applying Donnell shell theory and modified variational principle, natural frequencies of joined spherical-cylindrical shells was investigated by He *et al*. (2020). Least-squares weighted residual approach was applied to solve the

*Corresponding author, Professor,
E-mail: masoudbabaei@eyc.ac.ir
**Co-corresponding author, Professor,
E-mail: wangxiangling402@163.com

ISSN: 2287-237X (Print), 2287-2388 (Online)

governing equations. By using Fourier- Chebyshev collocation approach, Lee (2018) presented natural frequency analysis of joined cylindrical-conical shells. Izadi *et al*. (2018) presented FEM and analytical solutions for natural frequencies of laminated joined conical shells based on Hamilton's principle and FSDT. Free vibration of a rotating shell structure constructed from joined cones was studied by Sarkheil *et al*. (2017). Soureshjani *et al*. (2020) investigated thermal conditions on the natural frequencies of joined conical-conical shells made of functionally graded carbon nanotube reinforced composites (FG CNT-RC) based on FSDT and Hamilton's principle. They used GDQ procedure to obtain the solution of the governing equations.

In terms of material, nowadays, there is a high request for great structural implementation and multifunctionality with excellent mechanical properties. The structures made of CNT and graphene platelet nanocomposites having valuable properties e.g. heat resistance, lightweight, excellent energy absorption, have been considerably used in different engineering (Rafiee *et al*. 2009, Zhao *et al*. 2010). Nano-fillers e.g. CNTs or GPLs into lightweight materials is employed as an effective and useful way to boost their mechanical properties. On the other hand, these nanoparticles will lead to keep their excellent potential for lightweight structures, if they disperse in the metal or polymer matrix. Comparing with CNTs, GPLs have revealed major abilities to choose a proper reinforcement volunteer due to they have great mechanical properties, a less expensive, a more special surface area and 2D geometry (Liu *et al*. 2013). To boost the efficiency and capability of structures, functionally graded reinforced graphene platelets structures have been suggested in the literature to determine the eligible mechanical properties by controlling the pattern and weight fraction of GPLs. Therefore, a lot of investigations have been performed about the behavior of structures which are made of these materials. In detailed, Mangalasseri *et al*. (2023) investigated vibration behavior based energy harvesting performance of magneto-electro-elastic beams reinforced with CNTs. Gauss's Law, Newton's Law and Faraday's Law were employed for deriving the governing equations of the structure. Arshid *et al*. (2021) used quasi-3D shear deformation theory, Hamilton's principle in conjunction with modified couple stress theory to study vibration response of FG microplates embedded by polymeric nanocomposite patches by considering hygrothermal effects. Garg *et al*. (2022b) employed Machine learning method to estimate the compressive strength of concrete containing nano silica. Djilali *et al*. (2022) studied large cylindrical deflection analysis of FG carbon nanotube-reinforced plates in thermal environment based on higher-order shear deformation theory (HSDT) and by using minimization of the total potential energy. Huang *et al*. (2021) applied a seven-unknown shear deformation theory and analytical procedure to investigate static stability analysis of carbon nanotube reinforced polymeric composite doubly curved micro-shell panels. Zerrouki *et al*. (2021) performed an investigation about the influences of nonlinear FG-CNT distribution on mechanical properties of functionally graded nano-composite beam based on HSDT. Mechanics of nanocomposites reinforced by wavy/ defected/ aggregated nanotubes was presented by Heidari *et al*. (2021). Deflections, stresses and free vibration studies of FG-CNT reinforced sandwich plates resting on Pasternak elastic foundation based on FSDT were reported by Bendenia *et al*. (2020). Al-Furjan *et al*. (2021) analyzed the stress and strain responses of the FG-GPL RC disk based on three-dimensional refined higher-order theory and by employing DQM as solution. Natural frequencies of viscoelastic multi-phase reinforced fully symmetric systems were presented by Al-Furjan *et al*. (2022). Al-Furjan *et al*. (2021) investigated vibration behavior of the imperfect sandwich higher-order disk with a lactic core using GDQ method. A computational framework for propagated waves in a sandwich doubly curved nanocomposite panel based on HSDT was presented by Al-Furjan *et al*. (2022). Bourada and his co-authors (2020) used FSDT beam theory to analyze stability and dynamic responses of CNT reinforced concrete beam resting on elastic-foundation. Mohammadimehr and Tounsi (2019) performed an investigation about nonlinear analysis of electro-magneto-elastic bending, buckling and vibration of viscoelastic micro-composite beam with geometrical imperfection by using FEM. Van Vinh and Tounsi (2022a) presented an analytical solution based on Navier solution for examining the role of spatial variation of the nonlocal parameter on the free vibration of functionally graded sandwich nanoplates based on classical nonlocal elasticity theory. Micro-structural/ geometric imperfection sensitivity on the vibration response of geometrically discontinuous bi-directional functionally graded plates with partial supports by using FEM was presented by Katiyar, Gupta and Tounsi (2022). Liu *et al*. (2022) employed third-order shear deformation theory in conjunction with Eringen nonlocal elasticity and a state-space method to investigate dynamics behavior of imperfect inhomogeneous nanoplate with exponentially-varying properties resting on viscoelastic foundation. Babaei *et al*. (2021) investigated stress wave propagation of FG porous joined truncated conical–cylindrical-conical shells reinforced by GPLs based on the Rayleigh-Ritz energy method, accompanied by the Finite element method. Van Vinh, Van Chinh and Tounsi (2022) studied static bending and buckling analysis of bi-directional functionally graded porous plates using an improved FSDT and FEM. Dynamic characteristics of mixture unified gradient elastic nanobeams was presented by Faghidian and Tounsi (2022). Predicting elemental stiffness matrix of FG nanoplates using Gaussian process regression based surrogate model in framework of layerwise model was presented by Garg *et al*. (2022a). Cuong-Le (2022) utilized isogeometric analysis (IGA) and Mindlin plate theory in conjuction with nonlocal strain gradient theory to investigate nonlinear bending analysis of porous sigmoid FGM nanoplates. Reddy *et al*. (2020) addressed several aspects such as preparation, structure–property relationships, properties of different types of clays and self-healing polymers, healing process of cracks in clays using polymers, crack healing mechanism, test methods of healing efficiency, properties of clays before and after healing of cracks, and their applications. Natural frequencies of functionally graded doubly curved nanoshells based on nonlocal FSDT with variable nonlocal

parameters was studied by Van Vinh and Tounsi (2022b). Free vibration analysis of FGM nanoplates embedded in an elastic medium based on four-unknown refined integral plate theory on aggregate with the nonlocal elasticity theory was investigated by Bouafia *et al*. (2021). Size-dependent vibration response of porous graded nanostructure with FEM and nonlocal continuum model based on a refined trigonometric HSDT was reported by Kumar *et al* (2021). Physical stability response of a single-layered graphene sheet resting on viscoelastic medium using nonlocal integral first-order theory was studied by Rouabhia *et al*. (2020). Pham and Nguyen (2022) investigated the influences of size-dependence on static response and natural frequencies of FG porous nanobeams based on refined higher-order deformation theory in conjunction with nonlocal strain gradient theory and by employing finite element method. Pham *et al*. (2021) examined a comprehensive investigation about static, free vibration, and buckling response of functionally graded porous nano-plates resting on the Parternak's two-parameter elastic medium foundation based on the strain approach and the Reissner-Mindlin theory. Finite element procedure was applied for solving the governing equation of the structure. An edge-based smoothed finite element method combined with the mixed interpolation of tensorial components technique based on HSDT for static and free vibration analyses of FG porous plates reinforced by GPLs was presented by Tran *et al*. (2020). Nguyen *et al*. (2022) analyzed the influences of partially supported elastic foundation on free vibration of FG porous plates based on FSDT finite element method. Pham *et al*. (2022a) applied isogeometric approach for free vibration analysis of bidirectional functionally graded plates in the fluid medium based on refined quasi three-dimensional plate theory. Pham *et al*. (2022b) studied dynamic instability behavior of magnetically embedded FG porous nanobeams based on refined higher-order shear deformation beam theory in conjunction with strain gradient theory and by employing finite element approach. Yang *et al*. (2017) studied postbuckling and buckling of FG multilayer GPL-RC beams applying FSDT and Halpin-Tsai micromechanics model. The torsional buckling response of FG porous nanocomposite cylindrical shells reinforced by GPLs was analyzed by Ghahfarokhi *et al*. (2019) by using FSDT, Halpin-Tsai model and Rayleigh-Ritz solution. Safarpour, Rahimi, and Alibeigloo (2020) tackled the static and dynamic behavior of GPL RC truncated shell and plate structures within the frameworks of theory of elasticity and DQM. Arefi *et al*. (2018) using a sinusoidal shear deformation theory, examined free vibration of FG GPL-RC nanoplate supporting on Pasternak foundation. Problem of nonlinear bending of FG GPL-RC beams applying von Kármán nonlinear strain-displacement relations and Timoshenko beam theory was conducted by Feng *et al*. (2017). Kiani (2018a) studied natural frequencies of GPL-RC laminated plates in thermal surroundings applying a non-uniform rational B- spline (NURBS) formulation based on Halpin–Tsai approach. Also, Kiani (2018b) applied NURBS to investigate thermal postbuckling behavior of GPL-RC laminated plates according to Halpin-Tsai approach. Song *et al*. (2017) studied dynamic analysis of FG GPL-RC plates according to FSDT and modified Halpin-Tsai micro-mechanics model. Dong *et al*. (2018) presented the nonlinear free vibration of FG GPL-RC cylindrical shells under axial load and spinning motion applying the Donnell's nonlinear shell theory. Ebrahimi *et al*. (2020) studied thermal vibration of nanocomposites plate made of graphene oxide powder-reinforced under various thermal conditions using HSDT. Nonlinear natural frequencies of GPL-RC dielectric beam were performed by Wang *et al*. (2019). Using FSDT and modified Halpin-Tsai approach, thermal buckling of FG GPL-RC annular sector plates was presented by Javani *et al*. (2020). Kiani (2020) investigated the influence of GPLs on the dynamic response of plates subjected to a moving load by using Ritz and Newmark methods. Jamalabadi *et al*. (2021) presented nonlinear vibration behavior of FG GPL-RC conical panels supporting on elastic foundation based on FSDT, Halpin-Tsai approach and employing 2D-GDQM. Javani *et al*. (2021) investigated nonlinear free vibration of FG-GPLRC circular plate resting on the nonlinear elastic support based on FSDT and using GDQM. Based on FSDT and by applying FEM, the effect of thermal environment and pressure on nonlinear vibration behavior of FG GPL-RC toroidal panels resting on nonlinear elastic foundation were presented by Bidzard *et al*. (2021).

Extended numerical solutions were applied to investigate the response of various structures. For example, Nguyen, Thai, and Nguyen-Xuan (2016) applied the FEM based on NURBS basis functions according to HSDT to study dynamic and static analyses of laminated composite plates. Guo *et al*. (2021) applied machine learning (ML) approach to investigate bending analysis of kirchhoff plates. An extended finite difference approach according to the peridynamic differential operator for various domains was presented by Shojaei *et al*. (2019). Phung-Van *et al*. (2020) analyzed FGM plates with porosity under thermo-hygro-mechanical conditions and dynamic loads based on HSDT and by employing isogeometric analysis (IGA) in conjunction with Newmark integration method. The static deflection analysis of composite conical shells was studied using isoparametric finite element (IFE) (Chaubey, Kumar, and Chakrabarti 2018). The nonlinear bending of macro and nano plates with three different thickness variations was presented by Dastjerdi and Beni (2019). It was considered that plate element rests on an elastic foundation and is subjected to nonuniform loading and thermal environment. The torsion analysis of circular cylinder structures under magnetostrictive effects was expressed by Zenkour (2014a). In addition, Zenkour (2014b) investigated the thermal stress analysis of piezoelectric hollow cylinders. Gupta and Talha (2018) searched the effects initial geometric imperfections on the stability analysis of FG plates using IFE. Also, the free vibration analysis of composite laminated plates was studied by Hachemi and Hamza-Cherif (2020) by using IFE and HSDT. The mechanics of small scaled composite plate and shell structures was also presented by using atomic size-dependent continuum mechanics theories. For instance, Zeighampourand Beni (2014) presented the cylindrical thin-shell model of simply supported single walled CNTs using modified strain gradient theory. Zeighampour *et al*. (2018) explained the wave propagation characteristics of cylindrical cylindrical thin-shells resting on viscoelastic Pasternak

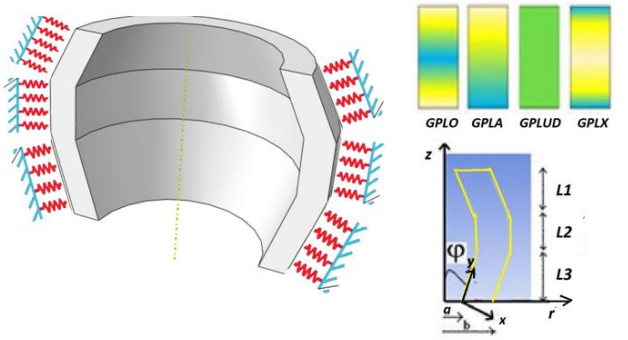

Fig. 1 Description of geometry of FG GPL–RC joined truncated conical-cylindrical-conical shell resting on elastic foundation for different GPL patterns through the thickness direction (x)

foundation via nonlocal strain gradient elasticity theory. Different numerical and analytical methods have been used for beams and plates having advanced composite material properties (Ait Atmane *et al*. 2015, Abdelaziz *et al*. 2017, Chen *et al*. 2017, Civalek *et al*. 2020a, b, Ebrahimi and Jafari 2016, Ebrahimi and Barati 2017, Hosseini and Zhang 2018). Also, bending, vibration and buckling analyses of nanobeams have been investigated in different studies (Kaghazian *et al*. 2017, Karami *et al*. 2018, Jalaei and Civalek 2019, Ebrahimi *et al*. 2020). In addition, mechanical, thermal and foundation effects on bending and frequency responses have been discussed by many researchers (Moradi and Mansouri 2012, Zemri *et al*. 2015, Kaddari *et al*. 2020, Tahouneh 2014, 2016, Wu and Liu 2016, Zhao *et al*. 2021).

The above literature shows that most of researches deal with simple shape structures such as beams, plates and cylindrical or conical shells, and the behavior of complicated shapes such as FG-GPL-RC joined shells are not investigated so far. Furthermore, in the most of previous studies, simple shell and plate theories rather than elasticity theory are used to model the problem. Application of 2D axisymmetric elasticity theory allows thickness stretching unlike simple shell theories, and this gives more accurate results, especially for thick shells. The application of joined shells is in many industries such as aerospace structures motivated the authors to study the free vibration behavior of these structures. Nowadays the GPL-RC is applied in aerospace industrial which lightweight structure has more significant value. Therefore, it motivates the authors to investigate the natural frequency of FG GPL-RC joined conical-cylindrical- conical shell for the first time. Therefore, in the present research, an efficient numerical model is conducted to study free vibration of joined truncated conical–cylindrical-conical shells reinforced by GPLs resting on Winkler elastic foundation. The multilayer graphene nano-composite shell is assumed with GPL-RC layers. Each separate layer consists of a combined of GPL as a nanofillers and isotropic polymer as a matrix in which GPLs are uniform or non- uniform dispersed in polymer matrix. The GPLs weight fraction varies as FG across the thickness. Four various kinds of volume fraction of FG GPL-RCs are supposed in this research and described in Section 2.2. FEM and Rayleigh- Ritz energy methods are applied to obtain and solve the governing motion equations. Details of 2D axisymmetric elasticity theory and FEM modeling are presented in Sections 3 and 4, respectively. Finally, in Section 5, the influence of different factors including GPL dispersion patterns, semi- vertex angle of cone, weight fraction of GPL nanofillers, stiffness of elastic foundation and boundary conditions on natural frequencies of joined shell have been investigated.

2. Governing equations

2.1 Definition of geometry

Consider a GPL–RC joined truncated conical-cylindrical-conical shell with total length L=L1+L2+L3 (L1 and L3 are the length of conical shells, and L2 is the length of cylindrical shell, respectively). h, *a*, *b* and φ are the thickness of structure, inner and outer radius of small base of cone and semi vertex angle, respectively that depicted in Fig.1. The shell is resting on Winkler-type elastic medium on the outer surface. The stiffness parameter of the elastic medium is considered as K_w. Also, various GPLs pattern is shown in Fig. 1.

Hence, the weight fraction of nano-filler (GPL) changes as functionally graded through the thickness (Wu *et al*. 2017). It is supposing that the structure is made of even number of layers, i.e., NL. Four various patterns of volume fraction of FG GPL-RCs are supposed: FG-A, O, X, and uniform pattern (UD). For UD, the GPL amount remains constant through any layer. Therefore, UD related to a homogeneous isotropic GPL-RC joined shell. In the FG patterns, the weight fraction of GPL varies linearly along the thickness of shell. For FG-X, the inner and outer layers are GPL maximum while this is different for FG-O where the mid-layers are GPL maximum. In addition, A-GPL RC where inner layers are rich and by distancing from the inner surface, the amount of it continuously decreased and in the outer surface where are GPL minimum. The equal weight fraction for various GPL dispersion can be obtained as following (Arefi *et al*. 2019a, b)

$$\begin{aligned} &U-GPLRCV_{GPL}^{(k)}=V_{GPL}^{*}\\ &X-GPLRCV_{GPL}^{(k)}\\ &=4V_{GPL}^{*}(0.5+\frac{\left|K-\frac{N_L+1}{2})\right|}{2+N_L}\\ &O-GPLRCV_{GPL}^{(k)}\\ &=4V_{GPL}^{*}((N_L+1)/2-|K-(N_L+1)/2)|/(2+N_L)\\ &A-GPLRCV_{GPL}^{(k)}=2V_{GPL}^{*}K/(N_L+1) \end{aligned} \quad (1)$$

Here $V_{GPL}^{(k)}$ shows the volume content of GPL in the k-th layer of the shell. In Eq. (1), k changes from 1 to N_L. Also V_{GPL}^{*} shows the total volume fraction of the structure, and may be obtained as following:

$$V_{GPL}^{*}=\frac{\Delta_{GPL}\rho_m}{\Delta_{GPL}\rho_m+\rho_{GPL}-\Delta_{GPL}\rho_{GPL}} \quad (2)$$

where ρ_{GPL} and ρ_m are the mass density of GPLs and matrix, respectively. And Δ_{GPL} is in terms of the weight fraction of the GPLs in the matrix. According to Halpin-

Tsai micromechanics model (Kiani 2019, Kiani and Żur 2022), elastic modulus of the nanocomposite E is expressed as:

$$E = \frac{3}{8}\left(\frac{1+\varepsilon_L^{GPL}\eta_L^{GPL}V_{GPL}}{1-\eta_L^{GPL}V_{GPL}}\right)E_m + \frac{5}{8}\left(\frac{1+\varepsilon_W^{GPL}\eta_W^{GPL}V_{GPL}}{1-\eta_W^{GPL}V_{GPL}}\right) \tag{3}$$

$$\varepsilon_L^{GPL} = \frac{2l_{GPL}}{t_{GPL}} \tag{4}$$

$$\varepsilon_W^{GPL} = \frac{2w_{GPL}}{t_{GPL}} \tag{5}$$

$$\eta_L^{GPL} = \frac{E_{GPL}-E_m}{E_{GPL}+\varepsilon_L^{GPL}E_m} \tag{6}$$

$$\eta_W^{GPL} = \frac{E_{GPL}-E_m}{E_{GPL}+\varepsilon_W^{GPL}E_m} \tag{7}$$

where E_{GPL} , E_m , l_{GPL}, W_{GPL} , t_{GPL} and V_{GPL} being the elasticity modulus of GPLs, the elasticity modulus of matrix, length, width, thickness of Nano-filler platelets, and the volume content of GPLs, respectively. The rule of mixture (Kiani and Żur 2022) is used to calculate the mass density and Poisson's ratio of the GPL-RC:

$$\rho = \rho_{GPL}V_{GPL} + \rho_m(1-V_{GPL}) \tag{8}$$

$$v = v_{GPL}V_{GPL} + v_m(1-V_{GPL}) \tag{9}$$

where υ_{GPL} and υ_m are the Poisson's ratio of GPL and matrix, respectively. The rigidity modulus G of the nanocomposite expresses as bellow:

$$G = \frac{E}{2(1+\upsilon)} \tag{10}$$

3. Deriving governing equations of motion

Consider a joined truncated conical-cylindrical-conical shell as depicted in Fig. 1. As obvious, the shell is 3-D while the geometry of the shell doesn't depend on the circumferential direction. Therefore, the shell equations can be reduced to 2D-axisymmetric elasticity equations. Consequently, the circumferential displacement, shear strains and stresses in rθ and θz planes vanishes. Thus, the governing equation in term of stresses $\sigma_{ij}(i,j)= r, \theta, z$ in axisymmetric cylindrical coordinates by omitting the body forces are expressed as following:

$$\sigma_{rr,r} + \frac{1}{r}(\sigma_{rr}-\sigma_{\theta\theta}) + \tau_{rz,z} = \rho\, u_{,tt} \tag{11}$$

$$\tau_{rz,r} + \sigma_{zz,z} + \frac{1}{r}\tau_{rz} = \rho\, v_{,tt} \tag{12}$$

The strain-displacement relations are as:

$$[\varepsilon] = \begin{bmatrix}\varepsilon_{rr}\\ \varepsilon_{\theta\theta}\\ \varepsilon_{zz}\\ \varepsilon_{rz}\end{bmatrix} = \begin{bmatrix} u_{,r}\\ \frac{1}{r}u\\ v_{,z}\\ \frac{1}{2}(u_{,z}+v_{,r})\end{bmatrix} \tag{13}$$

In which u and v are the radial and axial directions. Eq. 13 can be introduced as:

$$[\varepsilon] = [d]\{f\},\ \{f\} = \begin{Bmatrix}u\\ v\end{Bmatrix},\ [d] = \begin{bmatrix}\frac{\partial}{\partial r} & 0\\ \frac{1}{r} & 0\\ 0 & \frac{\partial}{\partial z}\\ \frac{1}{2}\frac{\partial}{\partial z} & \frac{1}{2}\frac{\partial}{\partial r}\end{bmatrix} \tag{14}$$

Matrix form of the stress-strain relation resulted from the Hooke's law as the following

$$[\sigma] = \begin{bmatrix}\sigma_{rr}\\ \sigma_{\theta\theta}\\ \sigma_{zz}\\ \tau_{rz}\end{bmatrix} = [D][\varepsilon] \tag{15}$$

where the coefficients of elasticity is as:

$$[D] = \frac{E}{(1+\upsilon)(1-2\upsilon)}\begin{bmatrix}1-\upsilon & \upsilon & \upsilon & 0\\ \upsilon & 1-\upsilon & \upsilon & 0\\ \upsilon & \upsilon & 1-\upsilon & 0\\ 0 & 0 & 0 & \frac{1-2\upsilon}{2}\end{bmatrix} = E\Lambda \tag{16}$$

The constant part of matrix D is defined as $\mathbf{\Lambda}$. For a shell that is clamped on its two end surfaces, the displacement boundary conditions are considered as:

B.C 1:

$$u, v(r,0) = u, v(r,L) = 0 \tag{17}$$

and for a shell which is clamped at its outer surface, one may write

B.C 2:

$$\mathrm{u, v(r_{out}, z)} = 0 \tag{18}$$

A combination of Eqs. (17)-(18) is related to a shell which is clamed at its two end edges and outer surface (B.C 3).

4. Applying finite element approach

In this part, for solving the governing motion equations of the structure, the finite element procedure is applied. By using the shape functions of quadratic six noded triangular element having two degrees of freedom for each node (u, v) in the axisymmetric cylindrical coordinate system, the displacement components for any element (e) is defined based on the approximation function matrix $\boldsymbol{N}$ and the displacement vector of nodes $\{\delta\}$ as:

$$\{q\}^{(e)} = N^e\ \{\delta\}^e \tag{19}$$

Applying Eq. (19) into Eq. (14) gives the strain matrix of

element (e) as following:

$$\{\varepsilon\}^{(e)} = \boldsymbol{B}^{(e)}\{\delta\}^{(e)}, \{\delta\}^{(e)} = \begin{bmatrix} U_1 \\ V_1 \\ . \\ . \\ . \\ U_6 \\ V_6 \end{bmatrix} \quad (20)$$

where $\boldsymbol{B}^{(e)} = [d]\boldsymbol{N}^{(e)}$. $\boldsymbol{N}^{(e)}$ and $\boldsymbol{B}^{(e)}$ are mentioned in the appendix.

The FE model of the structure may be derived by applying the Rayleigh-Ritz energy formulation as following. There are different textbooks (Zienkiewicz *et al*. 2005) explained this method in detail. The potential energy function of the joined shell including the strain and kinetic energies of shell and potential energy due to the Winkler elastic foundation is as:

$$\Pi^{(e)} = \frac{1}{2}\int_{V^{(e)}} \left(\boldsymbol{\varepsilon}^{(e)}\right)^T \boldsymbol{\sigma}^{(e)} dV + \int_{V^{(e)}} \rho \left(\boldsymbol{q}\right)^T \ddot{\boldsymbol{q}}^{(e)} dV +$$
$$\frac{1}{2}\left(\int_{A^{(e)}} K_w {w_n}^2 dA\right)_{x=r_{out}} = \frac{1}{2}\int_{V^{(e)}} \left(\boldsymbol{\delta}^{(e)}\right)^T \mathbf{B}^T E\, \boldsymbol{\Lambda}\mathbf{B}\boldsymbol{\delta}^{(e)} dV +$$
$$\int_{V^{(e)}} \left(\boldsymbol{\delta}^{(e)}\right)^T \rho \mathbf{N}^T \mathbf{N} \ddot{\boldsymbol{\delta}}^{(e)} dV +$$
$$\frac{1}{2}\left(\int_{A^{(e)}} K_w \mathbf{N}^T \Psi \Psi^T \mathbf{N}\, dA\right)_{x=r_{out}} \quad (21)$$
$$w_n = u\cos\varphi + v\sin\varphi = \boldsymbol{q}^T \begin{bmatrix} \cos\varphi \\ \sin\varphi \end{bmatrix} = \boldsymbol{q}^T \Psi = \left(\mathbf{N}\boldsymbol{\delta}^{(e)}\right)^T \Psi$$

$\Psi = \begin{bmatrix} cos\ \varphi \\ sin\varphi \end{bmatrix}$ For cylindrical section of joined shell:

$$\Psi = \begin{bmatrix} 1 \\ 0 \end{bmatrix}$$

w_n is the component of displacement field normal to the outer surface of the shell (i.e., along the x direction) and Ψ is a transformation vector . Influence of Winkler-type elastic foundations on the outer radius of the shell is also presented in the potential energy (third term). Minimization of potential energy of joined shell gives the following relations:

$$\frac{\partial \Pi^{(e)}}{\partial \left(\boldsymbol{\delta}^{(e)}\right)^T} = 0$$
$$\Rightarrow \left(\int_{V^{(e)}} \rho \mathbf{N}^T \mathbf{N} dV\right)\ddot{\boldsymbol{\delta}}^{(e)} + \left(\int_{V^{(e)}} \mathbf{B}^T E\boldsymbol{\Lambda}\mathbf{B} dV\right)\boldsymbol{\delta}^{(e)} \quad (22)$$
$$+ \left(\int_{A^{(e)}} K_w \boldsymbol{N}^T \Psi \Psi^T \boldsymbol{N}\, dA\right)_{x=r_{out}} \boldsymbol{\delta}^{(e)} = \mathbf{0}$$

Then by utilizing this procedure to achieve the governing motion equations, the stiffness and mass element matrices are as the following:

$$\mathbf{K}^{(e)} = \int_{V^{(e)}} \mathbf{B}^T E\boldsymbol{\Lambda}\mathbf{B} dV$$
$$+\left(\int_{A^{(e)}} K_w \boldsymbol{N}^T \Psi \Psi^T \boldsymbol{N}\, dA\right)_{x=r_{out}} \quad (23)$$

$$\boldsymbol{M}^{(e)} = \int_{V^{(e)}} \rho \boldsymbol{N}^T \boldsymbol{N}\, dV \quad (24)$$

The first term of stiffness matrix belongs to the strain energy of the shell and the second ones corresponds to the elastic foundation. The global equations of motion for GPL-RC joined truncated conical–cylindrical-conical shell reinforced by GPLs resting on elastic foundation after assembling the element matrices can be introduced as:

$$[\boldsymbol{M}]\{\ddot{\delta}\} + [\boldsymbol{K}]\{\delta\} = 0 \quad (25)$$

Solving the system of eigenvalue in Eq. (26), the natural frequencies and mode shapes of FG GPL-RC joined shell are obtained.

$$([\boldsymbol{K}] - [\boldsymbol{M}]\omega^2)\{\delta\} = 0 \quad (26)$$

5. Result and discussion

5.1 Verification

Natural frequency of FG GPL-RC joined truncated conical–cylindrical-conical shell reinforced by GPLs has not been studied yet. Hence, for confirming the numerical results of the present study, we compared the present results for joined truncated conical–cylindrical-conical shell made of homogenous material extracted from ANSYS WORKBENCH commercial FEM software. For this target, it is sufficient to consider γ_{GPL}= 0 % in the present study. Besides, the following material property and geometry are considered:

Geometry: a = 1(m), b =1.5 (m), L_1=0.5 (m), L_2=0.5 (m), L_3=0.5 (m), φ = 15°

Material property: $E = 200$ GPa, $\rho = 7850\ \frac{kg}{m^3}$, υ =0.3

A compression between the results of the present study and ANSYS WORKBENCH is shown in Fig. 2 and Table 1, and it shows excellent agreement. Also, to obtain convergent results (*nr*, *nz*)=(12*39) elements along the radial and axial directions are considered.

5.2 Numerical results and discussions

At this part, the results of natural frequencies of FG GPL- RC joined truncated conical–cylindrical shell have been obtained numerically. The effects of various parameters including boundary conditions, GPLs distribution, the weight fraction of GPL, stiffness of elastic foundation, various semi vertex angle and length ratio have been studied. Here the material and geometrical properties of the FG GPL-RC joined truncated conical-cylindrical-conical shell are presented:

• Description of material property: At this part, For GPL: E_{GPL} = 1.01 TPa, ρ_{GPL} = 1062.5 $\frac{kg}{m^3}$, ρ_{GPL} =0.186 , W_{GPL}= 1.5 μm, l_{GPL} = 2.5 μm, t_{GPL} = 1.5 nm for GPLs. For matrix E_m = 3 GPa, ρ_m = 1200 $\frac{kg}{m^3}$, υ_m = 0.34. Epoxy is considered as matrix

• Geometrical properties: a=1 (m), b=1.5 (m), L1=1 (m), L2=1 (m), L3=1 (m), φ = 15°

Firstly, results for the case that the shell is not supported by elastic foundation are presented. Table 2 indicates the effect of weight fraction of GPLs on the natural frequencies

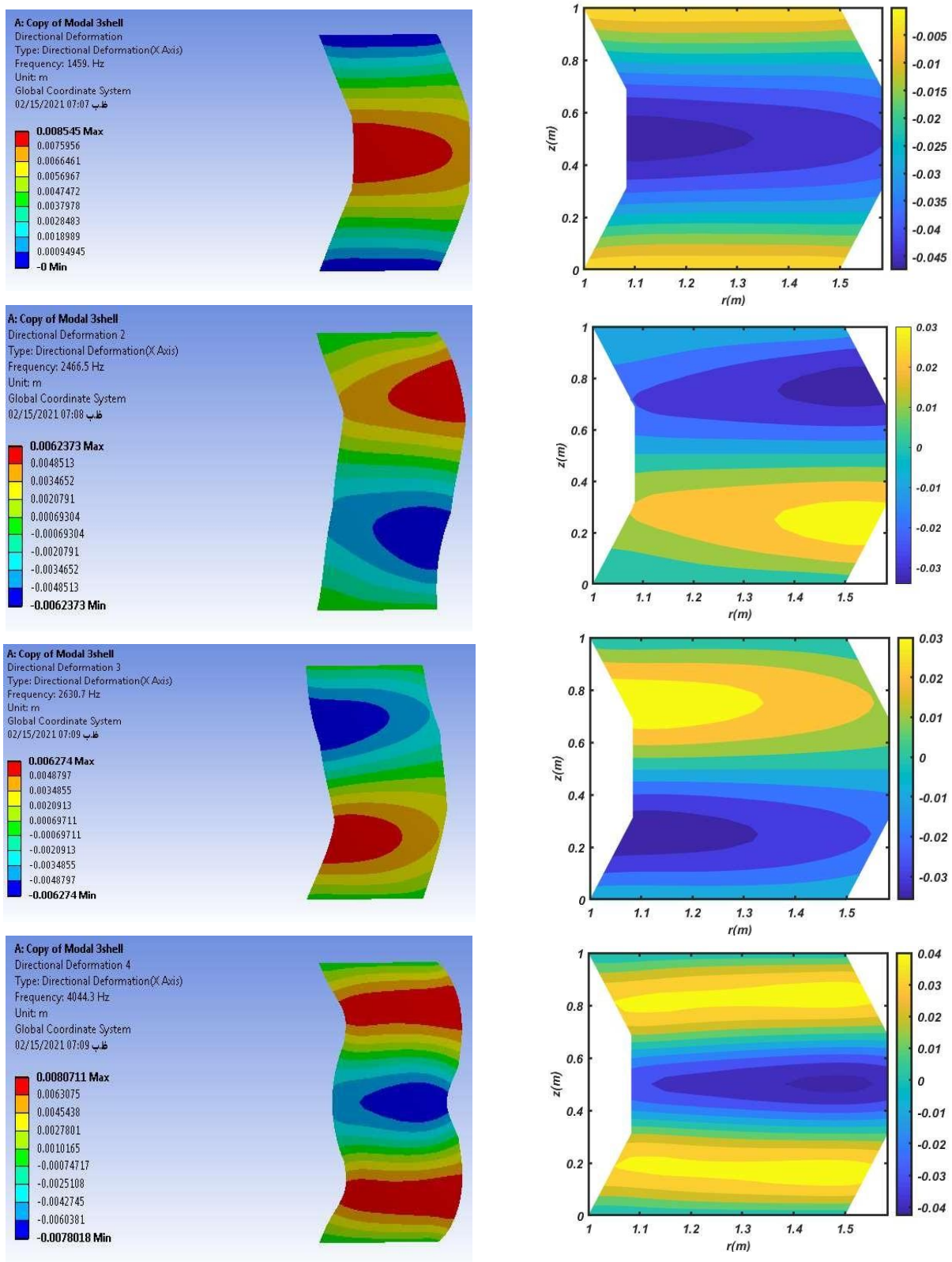

(a) ANSYS WORKBENCH (b) Present study

Fig. 2 Comparison of first four mode shapes between present study and ANSYS WORKBENCH

of the structure for B.C 1 for various GPL distributions. It is evident that by increasing the weight fraction of GPLs, the stiffness of shell increases, and consequently the natural frequencies of the shell are significantly increased (approximately up to 200%) while the mass of the shell varies a little. This point can be beneficial for aerospace components where the high strength and low weight are very vital. Also, the maximum natural frequencies belong to

Table 1 Comparative study for first four natural frequencies of joined shell between present study and ANSYS workbench

Natural frequency	ω1	ω2	ω3	ω4
Present	1463	2484	2657	4096
ANSYS WORKBENCH	1459	2466	2630	4044

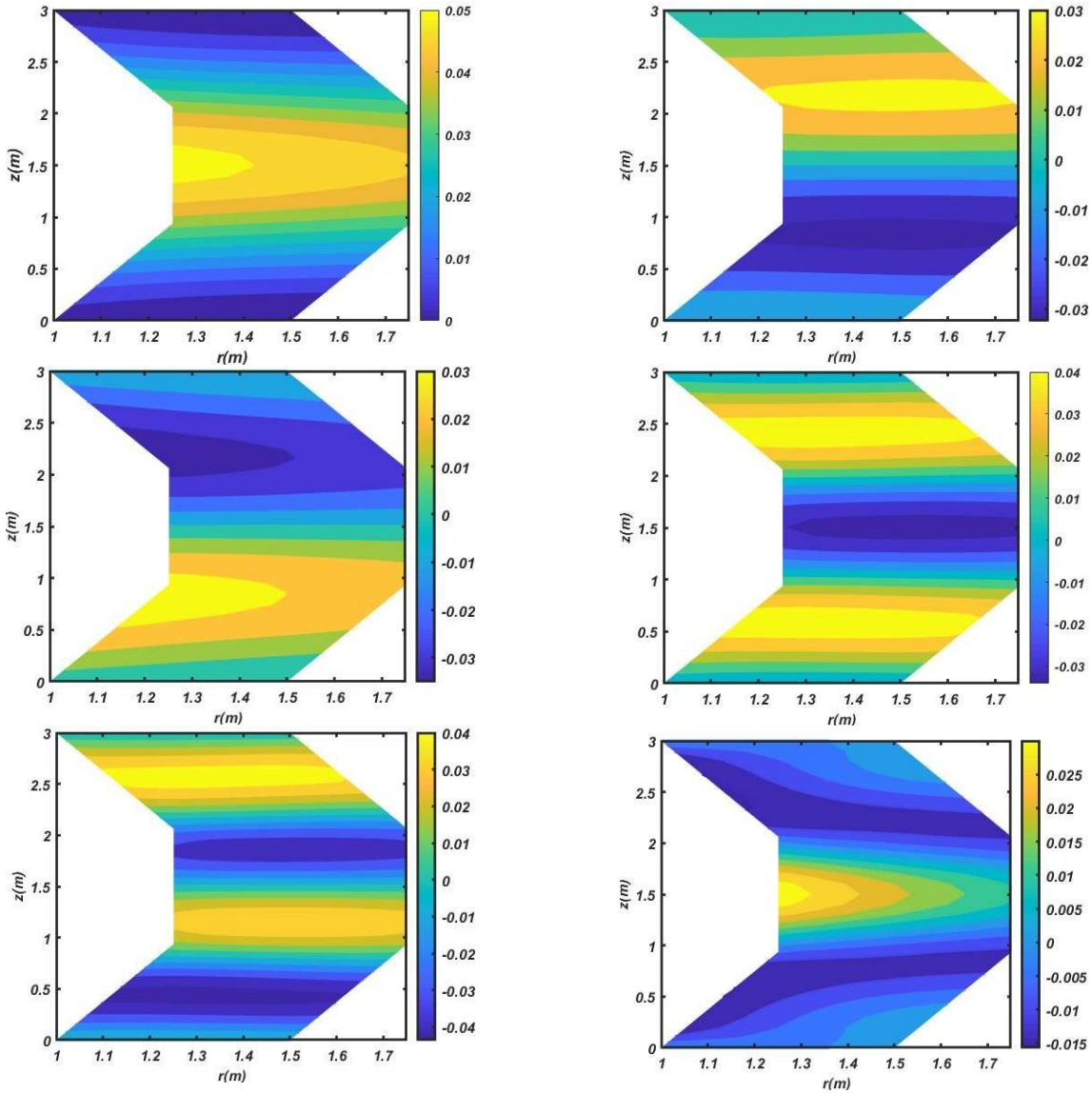

Fig. 3 The first six mode shapes of shell (GPLX, B.C 1, $\gamma_{GPL} = 0 \cdot 01$, $\varphi = 15°$)

GPLX, GPLO, GPLUD and GPLA, respectively. It means that the stiffness of the shell will be the most when the GPLs are more dispersed around the inner and outer surfaces of the shell. In addition, the effect of increasing weight fraction of GPLs on GPLX is more than other GPL pattern. It means that dispersing the GPLs around the inner and outer surface of the shell and with $\gamma_{GPL} = 0 \cdot 01$ is desirable for obtaining the maximum stiffness of the shell.

Table 3 shows the effect semi-vertex angle of the cone on the natural frequencies of the structure for different GPL distribution. By increasing the semi vertex angle, the natural frequencies are decreased. The important point is that in $\varphi = 60°$, the maximum natural frequencies belong to GPLO while in another semi vertex angles, the maximum natural frequencies are for GPLX. Table 4 indicates the influence of various boundary conditions on natural frequencies of structure for different GPL distributions. The maximum natural frequencies are for BC3, BC2, BC1, respectively. Results denote that the GPLO and BC3 provides the most rigidity that causes the most natural frequencies among different BC and GPL patterns. Table 5 indicates the influence of length ratio of the shell (length of conical shell per cylindrical shell) on natural frequencies for different GPL distributions. It is clear that the length ratio of the structure has not considerable effect on the natural frequencies of structure. However, by increasing the length

Table 2 The influence of various weight fraction of nanofillers and GPL distribution on natural frequencies of FG GPL-RC joined conical-cylindrical –conical shell (B.C 1)

GPL PATTERN	γ_{GPL}	ω1	ω2	ω3	ω4	ω5	ω6
GPLX	0	205	213	300	357	494	551
	0.005	431	432	590	720	987	1049
	0.01	570	574	777	946	1295	1372
GPLO	0	205	213	300	357	494	551
	0.005	405	420	629	696	972	1161
	0.01	535	550	840	898	1247	1530
GPLUD	0	205	213	300	357	494	551
	0.005	335	348	489	583	807	899
	0.01	427	443	623	743	1028	1146
GPLA	0	205	213	300	357	494	551
	0.005	324	338	498	561	783	921
	0.01	410	425	636	704	982	1174

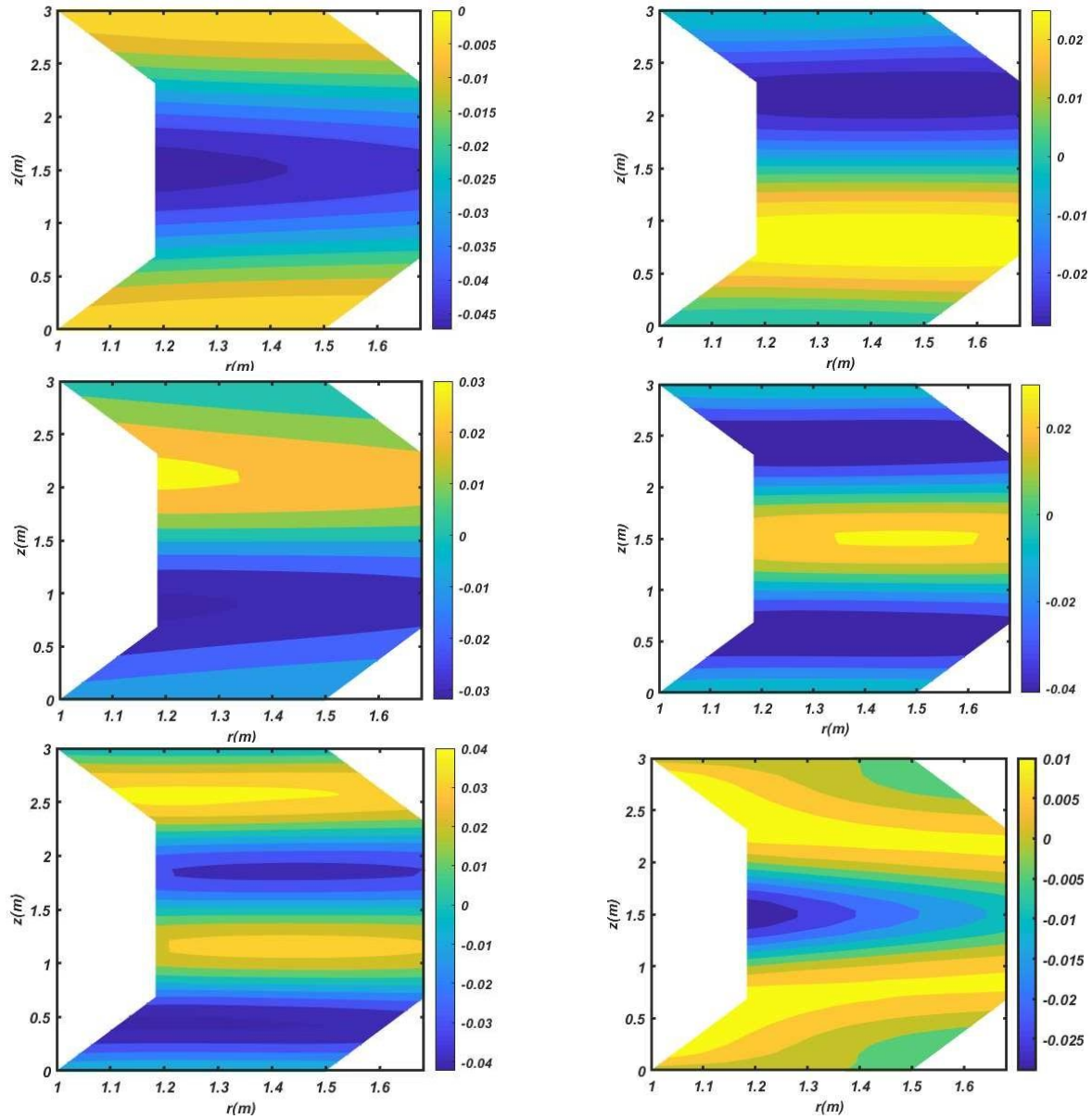

Fig. 4 The first six mode shapes of shell (GPLX, B.C 1, $\gamma_{GPL} = 0 \cdot 01$, $\varphi = 15°$, L2=2L1)

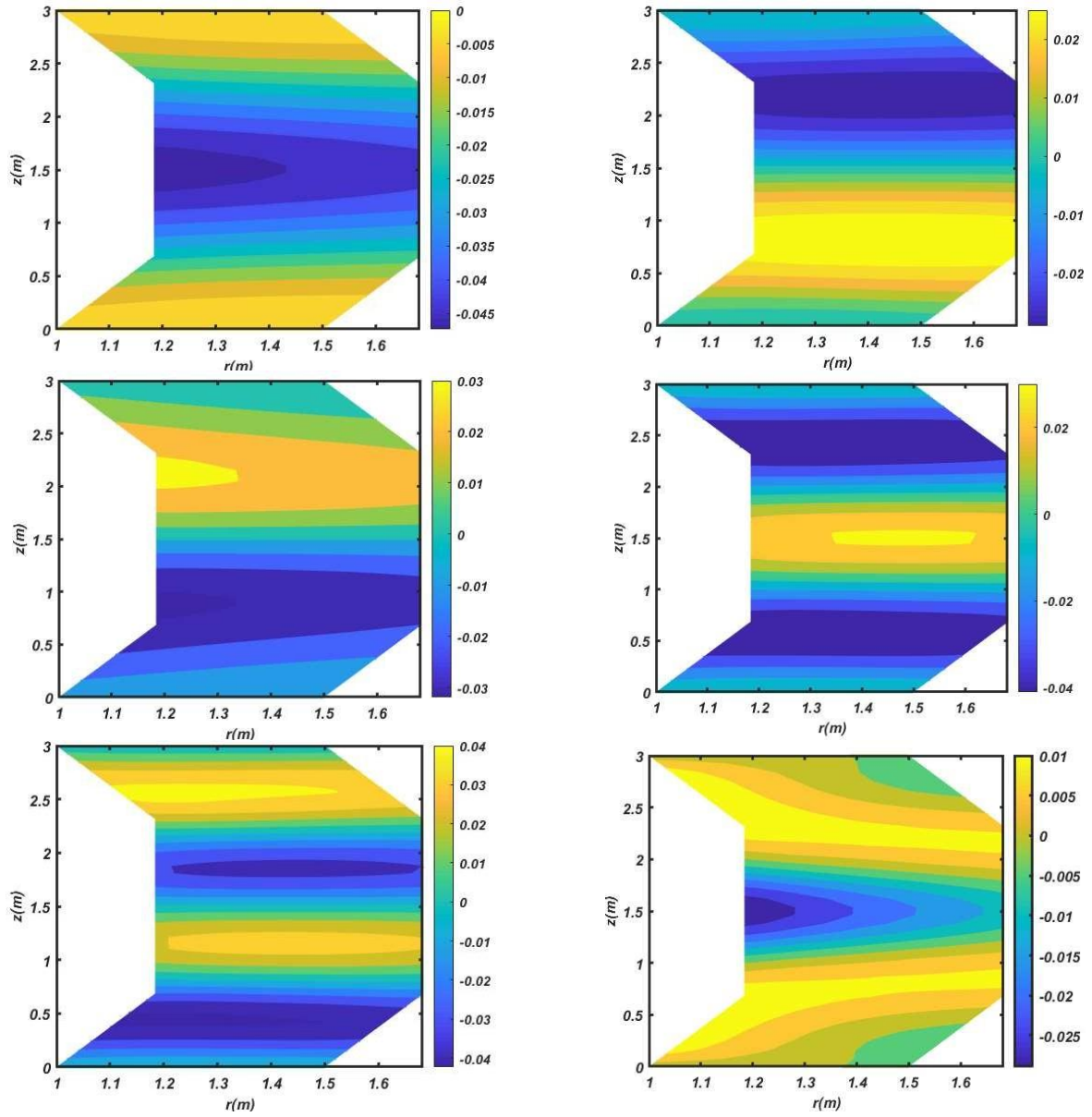

Fig. 5 The first six mode shapes of shell (GPLX, B.C 1, γ_{GPL} = 0 · 01, φ = 15°, ,L2=5 L1)

Table 3 Effect of semi vertex angles on the natural frequencies FG GPL-RC joined conical-cylindrical –conical shell (B.C 1, $\boldsymbol{\gamma GPL}$=0.01)

GPL PATTERN	φ	ω1	ω2	ω3	ω4	ω5	ω6
GPLX	0	632	686	799	1013	1356	1422
	30	437	543	717	855	1200	1316
	60	179	401	495	642	899	1175
GPLO	0	574	658	827	970	1329	1525
	30	428	521	787	825	1180	1499
	60	184	401	529	625	891	1230
GPLUD	0	465	525	631	790	1073	1166
	30	345	408	579	675	956	1099
	60	143	306	392	502	711	943
GPLA	0	441	505	631	748	1025	1167
	30	330	398	598	636	911	1141
	60	141	305	402	480	685	939

Table 4 Natural frequencies of FG GPL-RC joined conical-cylindrical –conical shell for different BC (φ=15˚, $\boldsymbol{\gamma GPL}$=0.01)

GPL PATTERN	BC	ω1	ω2	ω3	ω4	ω5	ω6
GPLX	1	570	574	777	946	1295	1372
	2	1016	1247	1702	1802	1854	1890
	3	1348	1849	1917	1955	2063	2218
GPLO	1	535	550	840	898	1247	1530
	2	1428	1486	1841	2222	2463	2724
	3	1776	2083	2338	2712	2804	2856
GPLUD	1	427	443	623	743	1028	1146
	2	1073	1149	1490	1824	1948	1978
	3	1321	1691	1977	1992	2108	2128
GPLA	1	410	425	636	704	982	1174
	2	1099	1145	1423	1737	1931	2097
	3	1361	1615	1836	2117	2151	2188

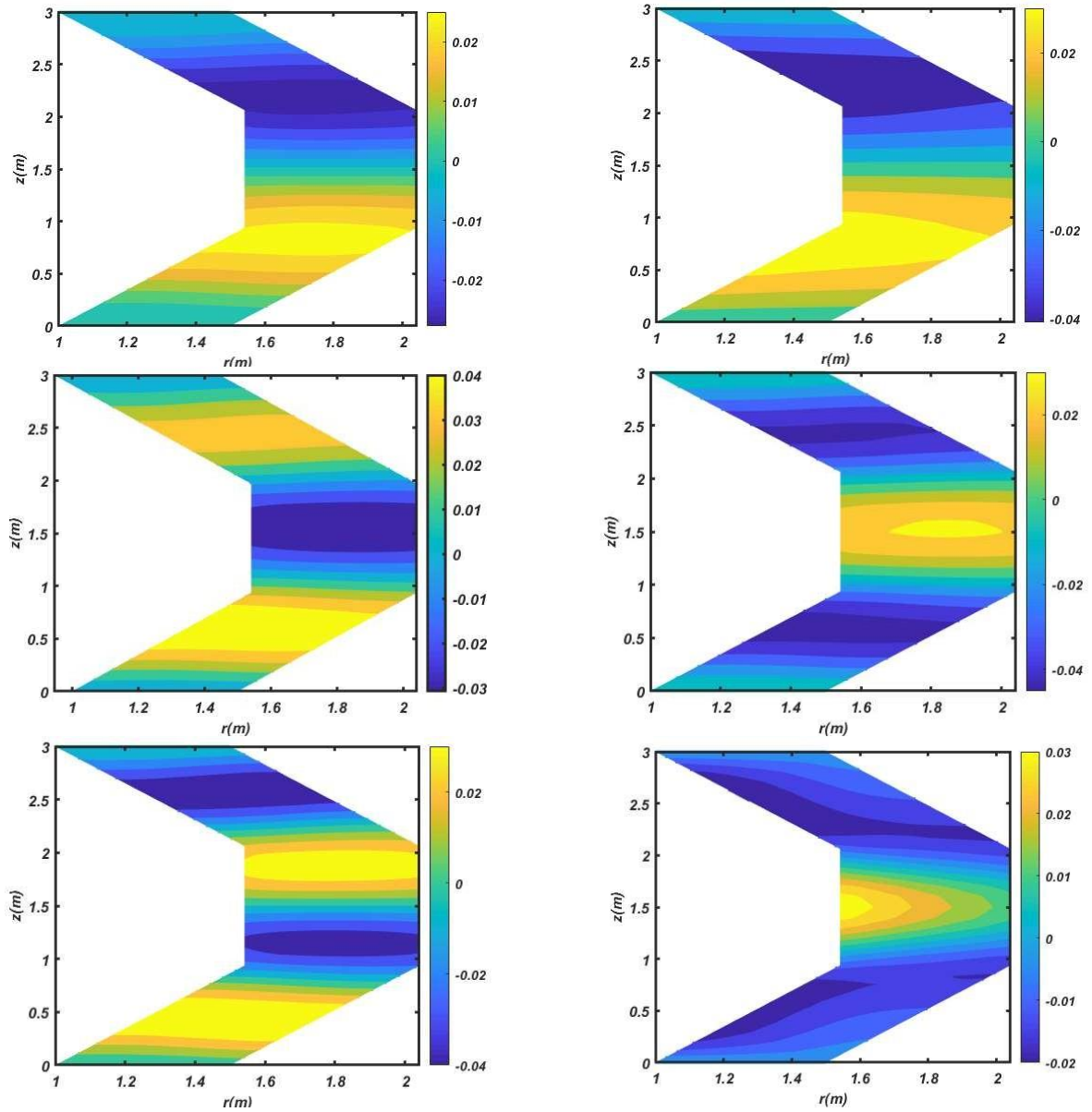

Fig. 6 The first six mode shapes of shell (GPLX, B.C 1, γGPL = 0 · 01, φ = 30°)

Table 5 Frequencies of FG GPL-RC joined conical-cylindrical –conical shell for different length ratio (φ=15˚, B.C 1, $\boldsymbol{\gamma GPL}$=0.01)

GPL PATTERN	*L*2/*L*1	**ω1**	**ω2**	**ω3**	**ω4**	**ω5**	**ω6**
GPLX	1	570	574	777	946	1295	1372
	2	581	586	805	969	1307	1347
	5	598	632	807	993	1336	1379
GPLO	1	535	550	840	898	1247	1530
	2	538	565	855	935	1298	1534
	5	548	602	840	948	1325	1524
GPLUD	1	427	443	623	743	1028	1146
	2	431	455	641	759	1043	1134
	5	442	485	639	773	1063	1148
GPLA	1	410	425	636	704	982	1174
	2	412	435	651	721	1000	1169
	5	421	463	641	731	1021	1164

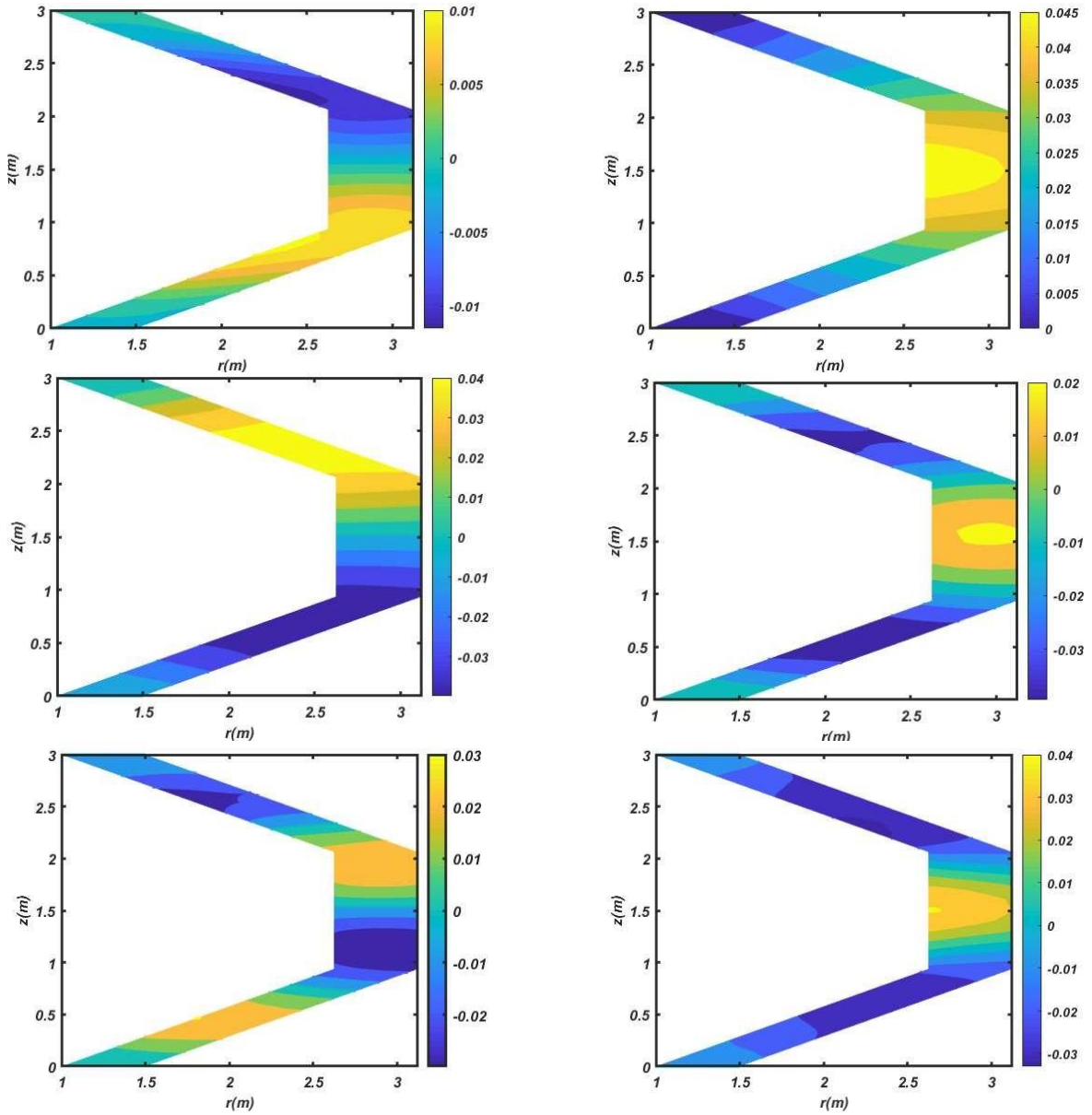

Fig. 7 The first six mode shapes of shell (GPLX, B.C 1, γGPL = 0 · 01, , φ = 60°)

Table 6 The influence of various stiffness of elastic foundation and GPL distribution on natural frequencies of FG GPL-RC joined conical-cylindrical –conical shell (B.C 1, γGPL = 0 · 01)

GPL PATTERN	Kw(GN/m$^{3)}$	**ω1**	**ω2**	**ω3**	**ω4**	**ω5**	**ω6**
GPLX	0	570	574	777	946	1295	1372
	1	594	640	808	972	1301	1374
	10	650	1027	1099	1255	1404	1517
GPLO	0	535	550	840	898	1247	1530
	1	584	604	865	936	1274	1536
	10	680	996	1130	1207	1404	1604
GPLUD	0	427	443	623	743	1028	1146
	1	472	510	662	780	1043	1147
	10	521	930	970	1099	1229	1291
GPLA	0	410	425	636	704	982	1174
	1	460	494	671	739	994	1175
	10	527	895	977	1054	1232	1273

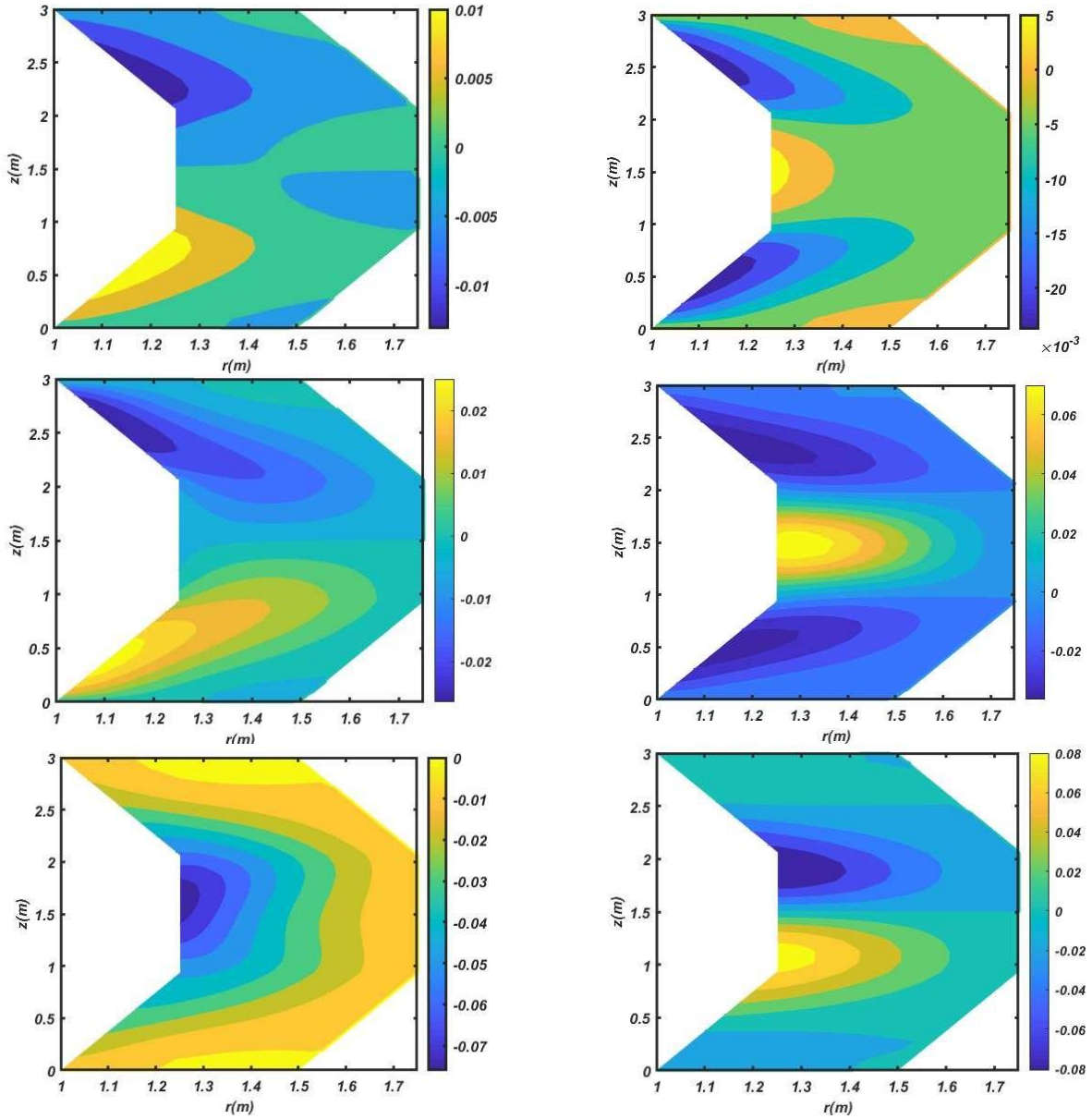

Fig. 8 The first six mode shapes of shell (GPLX, γGPL = 0 · 01, φ = 15°, BC3)

ratio of structure, the natural frequencies are increased. The first six mode shapes of shell for various length ratio are shown in Fig. 3 ($L_1 = L_2$), Fig. 4 ($L_1 = 2\ L_2$) and Fig. 5 ($L_1 = 5\ L_2$). The first six mode shapes of shell with B.C 1 for different semi vertex angle φ = 30°, 60° are shown in Figs. 6-7, respectively. Also, the first six mode shapes of shell with B.C 3 are shown in Fig. 8.

Now, the effects of considering elastic foundation on the natural frequencies of the shell are presented. Table 6 shows the effect of elastic foundation stiffness on the frequencies of FG-FGP RC joined shell with B.C 1, φ = 15° and $\gamma_{GPL} = 0 \cdot 01$ for various GPLs pattern. As it can be seen in this table, by increasing the stiffness of elastic foundation, the natural frequencies are considerably increased, especially for first four mode shapes.

6. Conclusions

Free vibration based on 2D axisymmetric elasticity theory by employing FEM according to Rayleigh-Ritz energy formulation in FG GPL-RC joined truncated conical–cylindrical-conical shell has been investigated for the first time. Applying 2D axisymmetric elasticity theory allows thickness stretching unlike simple shell theories, and this gives more accurate results, especially for thick shells. Also, for deriving more accurate results, higher order quadratic elements are used to mesh the solution domain. In addition, governing equations are developed for the shells supported on Winkler elastic foundation. The influences of various GPL distribution, weight fraction of GPL, semi vertex angle, boundary condition, stiffness of elastic foundation and length ratio on free vibration of structure have been studied that can be concluded as bellow:

• The B.C 3 has the most natural frequencies than other boundary conditions.

• GPLO and BC3 provide the most rigidity that causes the most natural frequencies among different BC and GPL patterns.

• In BC 1, for $\varphi = 0°$ and $\varphi = 30°$, GPLX pattern gives the most natural frequencies than GPLO, while in $\varphi = 60°$ the maximum natural frequency belongs to GPLO.

• Increasing the weigh fraction of nanofillers will increase natural frequencies approximately up to 200%, besides the influences of it on GPLX is more than other GPL pattern.

• The length ratio of shell has not considerable effect on natural frequencies of the structure.

• By increasing the stiffness of elastic foundation, the natural frequencies of joined shell considerably are increased, especially for first four mode shapes.

Acknowledgment

This work was supported by the National Science Fund for Distinguished Young Scholars (Grant number: 61525107).

References

Abdelaziz, H.H., Meziane, M.A.A, Bousahla, A.A., Tounsi, A., Mahmoud, S.R. and Alwabli, A.S. (2017), "An efficient hyperbolic shear deformation theory for bending, buckling and free vibration of FGM sandwich plates with various boundary conditions", *Steel Compos. Struct.*, **25**(6), 693-704. http://doi.org/10.12989/scs.2017.25.6.693.

Al-Furjan, M.S.H., Habibi, M., Ghabussi, A., Safarpour, H., Safarpour, M. and Tounsi, A. (2021), "Non-polynomial framework for stress and strain response of the FG-GPLRC disk using three-dimensional refined higher-order theory", *Eng. Struct.*, **228**, 111496. https://doi.org/10.1016/j.engstruct.2020.111496

Al-Furjan, M. S. H., Habibi, M., Shan, L. and Tounsi, A. (2021), "On the vibrations of the imperfect sandwich higher-order disk with a lactic core using generalize differential quadrature method", *Compos. Struct.*, **257**, 113150. https://doi.org/10.1016/j.compstruct.2020.113150

Al-Furjan, M.S.H., Habibi, M., Jung, D.W., Sadeghi, S., Safarpour, H., Tounsi, A. and Chen, G. (2022), "A computational framework for propagated waves in a sandwich doubly curved nanocomposite panel", *Eng. Struct.*, **38**(2), 1679-1696. https://doi.org/10.1007/s00366-020-01130-8

Al-Furjan, M.S.H., Habibi, M., Ni, J., Jung, D.W. and Tounsi, A. (2022), "Frequency simulation of viscoelastic multi-phase reinforced fully symmetric systems", *Eng. Struct.*, **38**(5), 3725-3741. https://doi.org/10.1007/s00366-020-01200-x

Alimirzaei, S., Mohammadimehr, M. and Tounsi, A. (2019), "Nonlinear analysis of viscoelastic micro-composite beam with geometrical imperfection using FEM: MSGT electro-magneto-elastic bending, buckling and vibration solutions", *Struct. Eng. Mech.*, **71**(5), 485-502. https://doi.org/10.12989/sem.2019.71.5.485

Ait Atmane, H., Tounsi, A., Bernard, F. and Mahmoud, S.R. (2015), "A computational shear displacement model for vibrational analysis of functionally graded beams with porosities", *Steel Compos. Struct.*, **19**(2), 369-384. https://doi.org/10.12989/scs.2015.19.2.369.

Arefi, M., Bidgoli, E.M.R., Dimitri, R. and Tornabene, F. (2018), "Free vibrations of functionally graded polymer composite nanoplates reinforced with graphene nano platelets", *Aerosp. Sci. Technol.*, **81**, 108-117. https://doi.org/10.1016/j.ast.2018.07.036

Arefi, M., Bidgoli, E.M.R., Dimitri, R., Bacciocchi, M. and Tornabene, F. (2019a), "Nonlocal bending analysis of curved nanobeams reinforced by graphene nanoplatelets", *Compos Part B: Eng.* **166**, 1-12. https://doi.org/10.1016/j.compositesb.2018.11.092

Arefi, M., Bidgoli, E.M.R. and Rabczuk, T. (2019b), "Effect of various characteristics of graphene nanoplatelets on thermal buckling behavior of FGRC micro plate based on MCST", *Eur. J. Mech. A Solids*, **77**, 103802. https://doi.org/10.1016/j.euromechsol.2019.103802

Arshid, E., Khorasani, M., Soleimani-Javid, Z., Amir, S. and Tounsi, A. (2021), "Porosity-dependent vibration analysis of FG microplates embedded by polymeric nanocomposite patches considering hygrothermal effect via an innovative plate theory", *Eng. Struct.*, **38**, 1-22. https://doi.org/10.1007/s00366-021-01382-y

Babaei, M., and Asemi, K. (2020a), "Stress analysis of functionally graded saturated porous rotating thick truncated cone", *Mech. Base Des. Struct.*,1-28. https://doi.org/10.1080/15397734.2020.1753536

Babaei, M. and Asemi, K. (2020b), "Static, dynamic and natural frequency analyses of functionally graded carbon nanotube annular sector plates resting on viscoelastic foundation", *SN*

Appl. Sci., **2**(10), 1-21. https://doi.org/10.1007/s42452-020-03421-7

Babaei, M., Kiarasi, F., Hossaeini Marashi, S.M., Ebadati, M., Masoumi, F., and Asemi, K. (2021), "Stress wave propagation and natural frequency analysis of functionally graded graphene platelet-reinforced porous joined conical–cylindrical–conical shell", *Waves Random Complex Med*., 1-33. https://doi.org/10.1080/17455030.2021.2003478

Bagheri, H., Kiani, Y., Bagheri, N. and Eslami, M.R. (2020), "Free vibration of joined cylindrical–hemispherical FGM shells", *Arch.Appl. Mech*., **90**, 2185-2199. https://doi.org/10.1007/s00419-020-01715-1

Bagheri, H., Kiani, Y. and Eslami, M.R. (2018), "Free vibration of joined conical–cylindrical–conical shells", *Acta Mechanica*, **229**(7), 2751-2764. https://doi.org/10.1007/s00707-018-2133-3

Bendenia, N., Zidour, M., Bousahla, A.A., Bourada, F., Tounsi, A., Benrahou, K.H., Bedia, E.A., Mahmoud, S.R. and Tounsi, A. (2020), "Deflections, stresses and free vibration studies of FG-CNT reinforced sandwich plates resting on Pasternak elastic foundation", *Comput. Concr*., **26**(3), 213-226. https://doi.org/10.12989/cac.2020.26.3.213

Bidzard, A., Malekzadeh, P. and Mohebpour, S (2021), "Influences of pressure and thermal environment on nonlinear vibration characteristics of multilayer FG-GPLRC toroidal panels on nonlinear elastic foundation", *Compos Struct*., **259**, 113503. https://doi.org/10.1016/j.compstruct.2020.113503

Bouafia, H., Chikh, A., Bousahla, A.A., Bourada, F., Heireche, H., Tounsi, A., Benrahou, K.H., Tounsi, A., Al-Zahrani, M.M. and Hussain., M. (2021), "Natural frequencies of FGM nanoplates embedded in an elastic medium", *Adv. Nano Res*., **11**(3), 239-249. https://doi.org/10.12989/anr.2021.11.3.239

Bourada, F., Bousahla, A.A., Tounsi, A., Bedia, E.A., Mahmoud, S.R., Benrahou, K.H. and Tounsi, A. (2020), "Stability and dynamic analyses of SW-CNT reinforced concrete beam resting on elastic-foundation", *Comput. Concr*., **25**(6), 485-495. https://doi.org/10.12989/cac.2020.25.6.485

Chaubey, A.K., A., Kumar and A., Chakrabarti (2018), "Novel shear deformation model for moderately thick and deep laminated composite conoidal shell", *Mech. Base Des. Struct*., **46**(5), 650668. https://doi.org/10.1080/15397734.2017.1422433

Chen, C.S., Liu, F.H. and Chen, W.R. (2017), "Vibration and stability of initially stressed sandwich plates with FGM face sheets in thermal environments", *Steel Compos. Struct*., **23**(3), 251-261. https://doi.org/10.12989/scs.2017.23.3.251

Civalek, O., Dastjerdi, S., Akbaş, S.D. and Akgöz, B. (2020a), "Vibration analysis of carbon nanotube-reinforced composite microbeams", *Math. Meth. Appl. Sci*., Special Issue Paper. https://doi.org/10.1002/mma.7069.

Civalek, O., Uzun, B., Yaylı, M.O. and Akgöz, B. (2020b), "Size-dependent transverse and longitudinal vibrations of embedded carbon and silica carbide nanotubes by nonlocal finite element method", *Eur. Phys. J. Plus*, **135**, 381. https://doi.org/10.1140/epjp/s13360-020-00385-w.

Cuong-Le, T., Nguyen, K.D., Le-Minh, H., Phan-Vu, P., Nguyen-Trong, P. and Tounsi, A. (2022), "Nonlinear bending analysis of porous sigmoid FGM nanoplate via IGA and nonlocal strain gradient theory", *Adv. Nano Res*., **12**(5), 441-455. https://doi.org/10.12989/anr.2022.12.5.441

Dastjerdi, S. and Beni, Y.T. (2019), "A novel approach for nonlinear bending response of macro and nanoplates with irregular variable thickness under nonuniform loading in thermal environment", *Mech. Base Des. Struct*., **47**(4), 453-478. https://doi.org/10.1080/15397734.2018.1557529

Djilali, N., A.A., Bousahla, A., Kaci, M.M., Selim, F., Bourada, A., Tounsi, A., Tounsi, K.H. Benrahou and S.R., Mahmoud. (2022), "Large cylindrical deflection analysis of FG carbon nanotube-reinforced plates in thermal environment using a simple integral HSDT", *Steel Compos. Struct*., **42**(6), 779-789. https://doi.org/10.12989/scs.2022.42.6.779

Dong, Y.H., B., Zhu, Y., Wang, Y.H., Li, and J., Yang (2018), "Nonlinear free vibration of graded grapheme reinforced cylindrical shells: Effects of spinning motion and axial load", *J Sound Vib*. **437**, 79-96. https://doi.org/10.1016/j.jsv.2018.08.036

Ebrahimi, F. and Jafari, A. (2016), "Thermo-mechanical vibration analysis of temperature-dependent porous FG beams based on Timoshenko beam theory", *Struct. Eng. Mech*., **59**(2), 343-371. https://doi.org/10.12989/sem.2016.59.2.343

Ebrahimi, F. and Barati, M.R. (2017), "Vibration analysis of embedded size dependent FG nanobeams based on third-order shear deformation beam theory", *Struct. Eng. Mech*, **61**(6), 721-736. https://doi.org/10.12989/sem.2017.61.6.721.

Ebrahimi, F., Karimiasl, M. and Selvamani, R. (2020), "Bending analysis of magneto-electro piezoelectric nanobeams system under hygro-thermal loading", *Adv. Nano Res*., **8**(3), 203-214. https://doi.org/10.12989/anr.2020.8.3.203.

Ebrahimi, F., Nouraei, M. and Dabbagh, A. (2020), "Thermal vibration analysis of embedded graphene oxide powder-reinforced nanocomposite plates", *Eng Comput*., **36**(3), 879-895. https://doi.org/10.1016/j.jsv.2018.08.036

Ebrahimi, F. and Seyfi, A. (2020), "Studying propagation of wave in metal foam cylindrical shells with graded porosities resting on variable elastic substrate", *Eng Comput*., **36,** 1-17. https://doi.org/10.1007/s00366-020-01069-w

Faghidian, A. and Tounsi, A. (2022), "Dynamic characteristics of mixture unified gradient elastic nanobeams", *Facta Univ. Series Mech. Eng*., **20**(3), 539-552. https://doi.org/10.22190/FUME220703035F

Feng, C., Kitipornchai, S. and Yang, J. (2017), "Nonlinear bending of polymer nanocomposite beams reinforced with non-uniformly distributed graphene platelets (GPLs)", *Compos. Part B Eng*., **110**, 132-140. https://doi.org/10.1016/j.compositesb.2016.11.024

Garg, A., Belarbi, M.O., Tounsi, A., Li, L., Singh, A. and Mukhopadhyay, T. (2022a), "Predicting elemental stiffness matrix of FG nanoplates using Gaussian Process Regression based surrogate model in framework of layerwise model", *Eng. Anal. Bound. Elem*., **143**, 779-795. https://doi.org/10.1016/j.enganabound.2022.08.001

Garg, A., Aggarwal, P., Aggarwal, Y., Belarbi, M.O., Chalak, H. D., Tounsi, A. and Gulia, R. (2022b), "Machine learning models for predicting the compressive strength of concrete containing nano silica", *Comput. Concr*., **30**(1), 33-42. https://doi.org/10.12989/cac.2022.30.1.033

Ghahfarokhi, D.S., Safarpour, M. and Rahimi, A.R. (2019), "Torsional buckling analyses of functionally graded porous nanocomposite cylindrical shells reinforced with graphene platelets (GPLs)", *Mech. Base Des. Struct*., 81-102. https://doi.org/10.1080/15397734.2019.1666723

Guo, H., Zhuang, X. and Rabczuk, T. (2021), "A deep collocation method for the bending analysis of Kirchhoff plate", *Comput. Mater. Continua*, **59**(2), 433-456. https://doi.org/10.32604/cmc.2019.06660

Gupta, A. and M., Talha (2018), "Influence of initial geometric imperfections and porosity on the stability of functionally graded material plates", *Mech. Base Des Struc*., **46**(6), 693-711. https://doi.org/10.1080/15397734.2018.1449656

Hachemi, M. and Hamza-Cherif, S.M. (2020), "Free vibration of composite laminated plate with complicated cutout", *Mech. Base Des. Struct*., **48**(2), 192–216. https://doi.org/10.1080/15397734.2019.1633341

He, Q., Dai, H.L., Gui, Q.F. and Li, J.J. (2020), "Analysis of vibration characteristics of joined cylindrical-spherical shells", *Eng Struct*., **218**, 110767. https://doi.org/10.1016/j.engstruct.2020.110767

Heidari, F., Taheri, K., Sheybani, M., Janghorban, M. and Tounsi, A. (2021), "On the mechanics of nanocomposites reinforced by wavy/defected/aggregated nanotubes", *Steel Compos. Struct.*, **38**(5), 533-545. https://doi.org/10.12989/scs.2021.38.5.533

Hosseini, S.M. and Zhang, C. (2018), "Elastodynamic and wave propagation analysis in a FG Graphene platelets-reinforced nanocomposite cylinder using a modified nonlinear micro-mechanical model", *Steel Compos. Struct.*, **27**(3), 255-271. https://doi.org/10.12989/scs.2018.27.3.255.

Huang, Y., Karami, B., Shahsavari, D. and Tounsi, A. (2021), "Static stability analysis of carbon nanotube reinforced polymeric composite doubly curved micro-shell panels", *Arch. Civil Mech. Eng.*, **21**(4), 139. https://doi.org/10.1007/s43452-021-00291-7

Irie, T., Yamada, G. and Muramoto, Y. (1984), "Free vibration of joined conical-cylindrical shells", *J Sound Vib.*, **95**(1), 31-39. https://doi.org/10.1007/s00707-018-2133-3

Izadi, M.H., Hosseini-Hashemi, S. and Korayem, M.H. (2018), "Analytical and FEM solutions for free vibration of joined cross-ply laminated thick conical shells using shear deformation theory", *Arch Appl Mech.*, **88**(12), 2231-2246. https://doi.org/10.1007/s00419-018-1446-y

Jalaei, M. and Civalek, O. (2019), "On dynamic instability of magnetically embedded viscoelastic porous FG nanobeam", *Int. J. Eng. Sci.*, **143**, 14-32. https://doi.org/10.1016/j.ijengsci.2019.06.013.

Jamalabadi, M.Y.A., Borji, P., Habibi, M. and Pelalak, R. (2021), "Nonlinear vibration analysis of functionally graded GPL-RC conical panels resting on elastic medium", *Thin Wall. Struct.*, **160**, 107370. https://doi.org/10.1016/j.tws.2020.107370

Javani, M., Kiani, Y. and Eslami, M.R. (2020), "Thermal buckling of FG graphene platelet reinforced composite annular sector plates", *Thin Wall. Struct.*, **148**, 106589. https://doi.org/10.1016/j.tws.2019.106589

Javani, M., Kiani, Y. and Eslami, M.R. (2021), "Geometrically nonlinear free vibration of FG-GPLRC circular plate on the nonlinear elastic foundation", *Compos. Struct.* **261**, 113515. https://doi.org/10.1016/j.compstruct.2020.113515

Jrad, H., Mars, J., Wali, M. and Dammak, F. (2019), "Geometrically nonlinear analysis of elastoplastic behavior of functionally graded shells", *Eng Comput.*, **35**(3), 833-847. https://doi.org/10.1007/s00366-018-0633-3

Kaddari, M., Kaci, A., Bousahla, A.A., Tounsi, A., Bourada, F., Tounsi, A., Bourada, F., Tounsi, A., Bedia, E.A.A. and Al-Osta, M.A. (2020), "A study on the structural behaviour of functionally graded porous plates on elastic foundation using a new quasi-3D model: Bending and free vibration analysis", *Comput. Concr. Int. J.*, **25**(1), 37-57. https://doi.org/10.12989/cac.2020.25.1.037

Kaghazian, A., Hajnayeb, A. and Foruzande, H. (2017), "Free vibration analysis of a piezoelectric nanobeam using nonlocal elasticity theory", *Struct. Eng. Mech.*, **61**(5), 617-624. https://doi.org/10.12989/sem.2017.61.5.617.

Karami, B., Janghorban, M., Shahsavari, D. and Tounsi, A. (2018), "A size-dependent quasi-3D model for wave dispersion analysis of FG nanoplates", *Steel Compos. Struct.*, **28**(1), 99-110. https://doi.org/10.12989/sem.2019.69.5.487.

Katiyar, V., Gupta, A., and Tounsi, A. (2022), "Microstructural/ geometric imperfection sensitivity on the vibration response of geometrically discontinuous bi-directional functionally graded plates (2D-FGPs) with partial supports by using FEM", *Steel Compos. Struct.*, **45**(5), 621-640. https://doi.org/10.12989/scs.2022.45.5.621

Kiani, Y. (2018a), "Isogeometric large amplitude free vibration of graphene reinforced laminated plates in thermal environment using NURBS formulation", *Comp. Meth. Appl. Mech. Eng.*, **332**, 86-101. https://doi.org/10.1016/j.cma.2017.12.015

Kiani, Y. (2018b), "NURBS-based isogeometric thermal post-buckling analysis of temperature dependent graphene reinforced composite laminated plates", *Thin Wall. Struct.*, **125**, 211-219. https://doi.org/10.1016/j.tws.2018.01.024

Kiani, Y. (2019), "Buckling of functionally graded graphene reinforced conical shells under external pressure in thermal environment", *Compos. Part B Eng.*, **156**, 128-137. https://doi.org/10.1016/j.compositesb.2018.08.052

Kiani, Y. (2020), "Influence of graphene platelets on the response of composite plates subjected to a moving load", *Mech. Base Des. Struct.*, 1-14.

Kiani, Y. and Żur, K.K. (2022), "Free vibrations of graphene platelet reinforced composite skew plates resting on point supports", *Thin Wall. Struct.*, **176**, 109363. https://doi.org/10.1016/j.tws.2022.109363

Kumar, Y., Gupta, A. and Tounsi, A. (2021), "Size-dependent vibration response of porous graded nanostructure with FEM and nonlocal continuum model", *Adv. Nano Res.*, **11**(1), 1-17. https://doi.org/10.12989/anr.2021.11.1.001

Lee, Y.S., Yang, M.S., Kim, H.S. and Kim, J.H. (2002), "A study on the free vibration of the joined cylindrical–spherical shell structures", *Comput. Struct.*, **80**(27-30), 2405-2414. https://doi.org/10.1016/S0045-7949(02)00243-2

Lee, J. (2018), "Free vibration analysis of joined conical-cylindrical shells by matched Fourier-Chebyshev collocation method", *J. Mech. Sci. Tech.*, **32**(10), 4601-4612. https://doi.org/10.1007/s12206-018-0907-0

Leissa, A.W. (1993), Vibration of Shells, American Institute of Physics, New York, U.S.A.

Liu, J., Yan, H., and Jiang, K. (2013), "Mechanical properties of graphene platelet-reinforced alumina ceramic composites", *Ceram. Int.*, **39**(6), 6215-6221. https://doi.org/10.1016/j.ceramint.2013.01.041

Liu, G., Wu, S., Shahsavari, D., Karami, B. and Tounsi, A. (2022), "Dynamics of imperfect inhomogeneous nanoplate with exponentially-varying properties resting on viscoelastic foundation", *Eur. J. Mech. A Solids*, **95**, 104649. https://doi.org/10.1016/j.euromechsol.2022.104649

Mangalasseri, A.S., Mahesh, V., Mukunda, S., Mahesh, V., Ponnusami, S.A., Harursampath, D. and Tounsi, A. (2023), "Vibration based energy harvesting performance of magneto-electro-elastic beams reinforced with carbon nanotubes", *Adv. Nano Res.*, **14**(1), 27-43. https://doi.org/10.12989/anr.2023.14.1.027

Moradi, S. and Mansouri, M.H. (2012), "Thermal buckling analysis of shear deformable laminated orthotopic plates by differential quadrature", *Steel Compos. Struct.*, **12**(2), 129-147. https://doi.org/10.12989/scs.2012.12.2.129

Nguyen, L.B., Thai, C.H., and Nguyen-Xuan, H. (2016), "A generalized unconstrained theory and isogeometric finite element analysis based on Bézier extraction for laminated composite plates", *Eng Comput.*, **32**(3), 457-475. https://doi.org/10.1007/s00366-015-0426-x

Nguyen, P.C., Pham, Q.H., Tran, T.T. and Nguyen-Thoi, T. (2022), "Effects of partially supported elastic foundation on free vibration of FGP plates using ES-MITC3 elements", *Ain Shams Eng. J.*, **13**(3), 101615. https://doi.org/10.1016/j.asej.2021.10.010

Patel, B.P., Ganapathi, M. and Kamat, S. (2000), "Free vibration characteristics of laminated composite joined conical-cylindrical shells", *J Sound Vib.*, **237**(5), 920-930. https://doi.org/10.1006/jsvi.2000.3018

Pham, Q.H., Nguyen, P.C., Tran, V.K. and Nguyen-Thoi, T. (2021), "Finite element analysis for functionally graded porous nano-plates resting on elastic foundation", *Steel Compos. Struct.*, **41**(2), 149-166. https://doi.org/10.12989/scs.2021.41.2.149

Pham, Q.H. and Nguyen, P.C. (2022), "Effects of size-dependence

on static and free vibration of FGP nanobeams using finite element method based on nonlocal strain gradient theory", *Steel Compos. Struct.*, ***45***(3), 331-348. https://doi.org/10.12989/scs.2022.45.3.331

Pham, Q.H., Nguyen, P.C., Tran, V.K. and Nguyen-Thoi, T. (2022a), "Isogeometric analysis for free vibration of bidirectional functionally graded plates in the fluid medium", *Defence Technol.*, **18**(8), 1311-1329. https://doi.org/10.1016/j.dt.2021.09.006

Pham, Q.H., Tran, V.K., Tran, T.T., Nguyen, P.C. and Malekzadeh, P. (2022b), "Dynamic instability of magnetically embedded functionally graded porous nanobeams using the strain gradient theory", *Alexandria Eng. J.*, **61**(12), 10025-10044. https://doi.org/10.1016/j.aej.2022.03.007

Phung-Van, P., Thai, C.H., Ferreira, A.J.M. and Rabczuk, T. (2020), "Isogeometric nonlinear transient analysis of porous FGM plates subjected to hygro-thermo-mechanical loads", *Thin-Walled Struct.*, **148**, 106497. https://doi.org/10.1016/j.tws.2019.106497

Qatu, M.S. (2004), *Vibration of Laminated Shells and Plates*, Elsevier, New York, U.S.A.

Qu, Y., Chen, Y., Long, X., Hua, H. and Meng, G. (2013), "A variational method for free vibration analysis of joined cylindrical-conical shells", *J. Vib. Control*, **19**(16), 2319-2334. https://doi.org/10.1177%2F1077546312456227

Rafiee, M.A., J.Z., Wang, H., Song, Z.Z., Yu, and N., Koratkar (2009), "Enhanced mechanical properties of nanocomposites at low graphene content", *ACS Nano*, **3**, 3884-3990. https://doi.org/10.1021/nn9010472

Reddy, K.R., El-Zein, A., Airey, D.W., Alonso-Marroquin, F., Schubel, P. and Manalo, A. (2020), "Self-healing polymers: Synthesis methods and applications", *Nano Struct. Nano Objects*, **23**, 100500. https://doi.org/10.1016/j.nanoso.2020.100500

Rouabhia, A., Chikh, A., Bousahla, A.A., Bourada, F., Heireche, H., Tounsi, A., Kouider H. and Tounsi, A. (2020), "Physical stability response of a SLGS resting on viscoelastic medium using nonlocal integral first-order theory", *Steel Compos. Struct.*, **37**(6), 695-709. https://doi.org/10.12989/scs.2020.37.6.695

Safarpour M., Rahimi, A.R. and Alibeigloo, A. (2020), "Static and free vibration analysis of graphene platelets reinforced composite truncated conical shell, cylindrical shell, and annular plate using theory of elasticity and DQM", *Mech. Base Des. Struct.*, **48**, 496-524. https://doi.org/10.1080/15397734.2019.1646137

Sarkheil, S., Foumani, M.S. and Navazi, H.M. (2017), "Free vibrations of a rotating shell made of p joined cones", *Int. J. Mech.Sci.*, **124**, 83-94. https://doi.org/10.1016/j.ijmecsci.2017.02.003

Shakouri, M. and M.A., Kouchakzadeh (2014), "Free vibration analysis of joined conical shells: Analytical and experimental study", *Thin Wall. Struct.*, **85**, 350-358. https://doi.org/10.1016/j.tws.2014.08.022

Shojaei, A., Galvanetto, U., Rabczuk, T., Jenabi, A. and Zaccariotto, M. (2019), "A generalized finite difference method based on the Peridynamic differential operator for the solution of problems in bounded and unbounded domains", *Comp Meth Appl Mech Eng.* **343**,100-126. https://doi.org/10.1016/j.cma.2018.08.033

Soedel, W. (2004), *Vibrations of Shells and Plates*, Marcel Dekker, New York., U.S.A. https://doi.org/10.3233/SAV-1995-2209

Song, M., Kitipornchai, S. and Yang, J. (2017), "Free and forced vibrations of functionally graded polymer composite plates reinforced with graphene nanoplatelets", *Compos Struct.*, **159**, 579-588. https://doi.org/10.1016/j.compstruct.2016.09.070

Soureshjani A.H., Talebitooti R. and Talebitooti, M. (2020), "Thermal effects on the free vibration of joined FG-CNTRC conical-conical shells", *Thin Wall. Struct.*, **156**, 106960. https://doi.org/10.1016/j.tws.2020.106960

Tahouneh, V. (2014), "Free vibration analysis of bidirectional functionally graded annular plates resting on elastic foundations using differential quadrature method", *Struct. Eng. Mech.*, **52**(4), 663-686. https://doi.org/10.12989/sem.2014.52.4.663.

Tahouneh, V. (2016), "Using an equivalent continuum model for 3D dynamic analysis of nanocomposite plates", *Steel Compos. Struct.*, **20**(3), 623-649. https://doi.org/10.12989/scs.2016.20.3.623.

Tran, T.V., Tran, T.D., Hoa Pham, Q., Nguyen-Thoi, T. and Tran, V.K. (2020), "An ES-MITC3 finite element method based on higher-order shear deformation theory for static and free vibration analyses of FG porous plates reinforced by GPLs", *Math. Probl. Eng.*, 1-18. https://doi.org/10.1155/2020/7520209

Van Vinh, P. and Tounsi, A. (2022a), "The role of spatial variation of the nonlocal parameter on the free vibration of functionally graded sandwich nanoplates", *Eng. Struct.*, **38**(5), 4301-4319. https://doi.org/10.1007/s00366-021-01475-8

Van Vinh, P. and Tounsi, A. (2022b), "Free vibration analysis of functionally graded doubly curved nanoshells using nonlocal first-order shear deformation theory with variable nonlocal parameters", *Thin Wall. Struct.*, **174**, 109084. https://doi.org/10.1016/j.tws.2022.109084

Van Vinh, P., Van Chinh, N. and Tounsi, A. (2022), "Static bending and buckling analysis of bi-directional functionally graded porous plates using an improved first-order shear deformation theory and FEM", *Eur. J. Mech. A Solids*, **96**, 104743. https://doi.org/10.1016/j.euromechsol.2022.104743

Wang, Y., Feng, C., Wang, X., Zhao, Z., Romero, C. S. and Yang, J. (2019), "Nonlinear free vibration of graphene platelets (GPLs)/ polymer dielectric beam", *Smart Mater. Struct.*, **28**(5), 055013. https://doi.org/10.1088/1361- 665X/ab0b51

Wu, H., Kitipornchai, S. and Yang, J. (2017), "Thermal buckling and postbuckling of functionally graded graphene nanocomposite plates", *Mater. Des.*, **132**, 430-441. https://doi.org/10.1016/j.tws.2017.05.006

Wu, C.P. and Liu, Y.C. (2016), "A state space meshless method for the 3D analysis of FGM axisymmetric circular plates", *Steel Compos. Struct.*, **22**(1), 161-182. https://doi.org/10.12989/scs.2016.22.1.161.

Yang, J., Wu, H. and Kitipornchai, S. (2017), "Buckling and postbuckling of functionally graded multilayer graphene platelet-reinforced composite beams", *Compos.Struct.*, **161**, 111-118. https://doi.org/10.1016/j.compstruct.2016.11.048

Zemri, A., Houari, M.S.A., Bousahla, A.A. and Tounsi, A. (2015), "A mechanical response of functionally graded nanoscale beam: an assessment of a refined nonlocal shear deformation theory beam theory", *Struct. Eng. Mech.*, **54**(4), 693-710. https://doi.org/10.12989/sem.2015.54.4.693

Zeighampour, H. and Beni, Y.T., (2014), "Cylindrical thin-shell model based on modified strain gradient theory", *Int. J. Eng. Sci.*, **78**, 27-47. https://doi.org/10.1016/j.ijengsci.2014.01.004

Zeighampour, H., Beni Y.T. and Dehkordi, M.B. (2018), "Wave propagation in viscoelastic thin cylindrical nanoshell resting on a visco-Pasternak foundation based on nonlocal strain gradient theory", *Thin Wall. Struct.*, **122**, 378-386. http://doi.org/10.1016/j.tws.2017.10.037

Zenkour, A.M. (2014a), "Torsional analysis of heterogeneous magnetic circular cylinder", *Steel Compos. Struct.*, **17**(4), 535-548. http://doi.org/10.12989/scs.2014.17.4.535

Zenkour, A.M. (2014b), "Exact solution of thermal stress problem of an inhomogeneous hygrothermal piezoelectric hollow cylinder", *Appl. Math. Modell.*, **38**(24), 6133-6143. https://doi.org/10.1016/j.apm.2014.05.028

Zerrouki, R., Karas, A., Zidour, M., Bousahla, A.A., Tounsi, A., Bourada, F., Tounsi, A., Benrahou, K.H. and Mahmoud, S.R. (2021), "Effect of nonlinear FG-CNT distribution on mechanical

properties of functionally graded nano-composite beam", *Struct. Eng. Mech.*, **78**(2), 117-124. https://doi.org/10.12989/sem.2021.78.2.117
Zhao, X., Q., Zhang, D., Chen and P., Lu (2010), "Enhanced mechanical properties of graphene based poly (vinyl alcohol) composites", *Macromolecules*, **43**, 2357–2363. https://doi.org/10.1021/ma902862u
Zhao, L.C., Chen, S.S., Xu, Y.P., Tahouneh, V. (2021), "Vibration analysis of damaged core laminated curved panels with functionally graded sheets and finite length", *Steel Compos. Struct.*, **38**, 477-496. https://doi.org/10.12989/scs.2021.38.5.477
Zienkiewicz, O.C., Taylor, R.L. and Zhu, J.Z. (2005), *The Finite Element Method: Its Basis and Fundamentals*, Elsevier.

CC

Appendix

$$\boldsymbol{N}=\begin{bmatrix} N_1 & 0 & N_2 & 0 & N_3 & 0 & N_4 & 0 & N_5 & 0 & N_6 & 0 \\ 0 & N_1 & 0 & N_2 & 0 & N_3 & 0 & N_4 & 0 & N_5 & 0 & N_6 \end{bmatrix}$$

$$N_1=\frac{(r_{23}(z-z_3)-z_{23}(r-r_3))(r_{46}(z-z_6)-z_{46}(r-r_6))}{(r_{23}z_{13}-z_{23}r_{13})(r_{46}z_{16}-z_{46}r_{16})}$$

$$N_2=\frac{(r_{31}(z-z_1)-z_{31}(r-r_1))(r_{54}(z-z_4)-z_{54}(r-r_4))}{(r_{31}z_{21}-z_{31}r_{21})(r_{54}z_{24}-z_{54}r_{24})}$$

$$N_3=\frac{(\mathrm{r}_{21}(\mathrm{z}-\mathrm{z}_1)-\mathrm{z}_{21}(\mathrm{r}-\mathrm{r}_1))(\mathrm{r}_{56}(\mathrm{z}-\mathrm{z}_6)-\mathrm{z}_{56}(\mathrm{r}-\mathrm{r}_6))}{(\mathrm{r}_{21}\mathrm{z}_{31}-\mathrm{z}_{21}\mathrm{r}_{31})(\mathrm{r}_{56}\mathrm{z}_{36}-\mathrm{z}_{56}\mathrm{r}_{36})}$$

$$N_4=\frac{(r_{31}(z-z_1)-z_{31}(r-r_1))(r_{23}(z-z_3)-z_{23}(r-r_3))}{(r_{31}z_{41}-z_{31}r_{41})(r_{23}z_{43}-z_{23}r_{43})}$$

$$N_5=\frac{(r_{31}(z-z_1)-z_{31}(r-r_1))(r_{21}(z-z_1)-z_{21}(r-r_1))}{(r_{31}z_{51}-z_{31}r_{51})(r_{21}z_{51}-z_{21}r_{51})}$$

$$N_6=\frac{\left(r_{21}(z-z_1)-z_{21}(r-r_1)\right)\left(r_{23}(z-z_3)-z_{23}(r-r_3)\right)}{(r_{21}z_{61}-z_{21}r_{61})(r_{23}z_{63}-z_{23}r_{63})}$$

$$\boldsymbol{B}=\begin{bmatrix} \frac{\partial N_1}{\partial r} & 0 & \frac{\partial N_2}{\partial r} & 0 & \frac{\partial N_3}{\partial r} & 0 & \frac{\partial N_4}{\partial r} & 0 & \frac{\partial N_5}{\partial r} & 0 & \frac{\partial N_6}{\partial r} & 0 \\ \frac{1}{r}N_1 & 0 & \frac{1}{r}N_2 & 0 & \frac{1}{r}N_3 & 0 & \frac{1}{r}N_4 & 0 & \frac{1}{r}N_5 & 0 & \frac{1}{r}N_6 & 0 \\ 0 & \frac{\partial N_1}{\partial z} & 0 & \frac{\partial N_2}{\partial z} & 0 & \frac{\partial N_3}{\partial z} & 0 & \frac{\partial N_4}{\partial z} & 0 & \frac{\partial N_5}{\partial z} & 0 & \frac{\partial N_6}{\partial z} \\ \frac{1}{2}\frac{\partial N_1}{\partial z} & \frac{1}{2}\frac{\partial N_1}{\partial r} & \frac{1}{2}\frac{\partial N_2}{\partial z} & \frac{1}{2}\frac{\partial N_2}{\partial r} & \frac{1}{2}\frac{\partial N_3}{\partial z} & \frac{1}{2}\frac{\partial N_3}{\partial r} & \frac{1}{2}\frac{\partial N_4}{\partial z} & \frac{1}{2}\frac{\partial N_4}{\partial r} & \frac{1}{2}\frac{\partial N_5}{\partial z} & \frac{1}{2}\frac{\partial N_5}{\partial r} & \frac{1}{2}\frac{\partial N_6}{\partial z} & \frac{1}{2}\frac{\partial N_6}{\partial r} \end{bmatrix}$$

$$\frac{\partial N_1}{\partial r}=\frac{-z_{23}[r_{46}[z-z_6]-z_{46}[r-r_6]]-z_{46}[r_{23}[z-z_3]-z_{23}[r-r_3]]}{[r_{23}z_{13}-z_{23}r_{13}][r_{46}z_{16}-z_{46}r_{16}]}$$

$$\frac{\partial N_1}{\partial z}=\frac{-r_{23}[r_{36}[z-z_6]-z_{36}[r-r_6]]-r_{46}[r_{13}[z-z_3]-z_{13}[r-r_3]]}{[r_{23}z_{13}-z_{23}r_{13}][r_{46}z_{16}-z_{46}r_{16}]}$$

$$\frac{\partial N_2}{\partial r}=\frac{-z_{31}[r_{54}[z-z_4]-z_{54}[r-r_4]]-z_{54}[r_{31}[z-z_1]-z_{31}[r-r_1]]}{[r_{21}z_{51}-z_{21}r_{51}][r_{21}z_{51}-z_{21}r_{43}]}$$

$$\frac{\partial N_2}{\partial z}=\frac{-r_{31}[r_{54}[z-z_4]-z_{54}[r-r_4]]+r_{54}[r_{21}[z-z_1]-z_{31}[r-r_1]]}{[r_{21}z_{21}-z_{31}r_{21}][r_{54}z_{24}-z_{54}r_{24}]}$$

$$\frac{\partial N_3}{\partial r}=\frac{-z_{21}[r_{56}[z-z_6]-z_{56}[r-r_6]]-z_{56}[r_{21}[z-z_1]-z_{21}[r-r_1]]}{[r_{21}z_{31}-z_{21}r_{31}][r_{56}z_{36}-z_{56}r_{36}]}$$

$$\frac{\partial N_3}{\partial z}=\frac{-r_{21}[r_{56}[z-z_6]-z_{56}[r-r_6]]-r_{56}[r_{21}[z-z_1]-z_{21}[r-r_1]]}{[r_{21}z_{31}-z_{21}r_{31}][r_{56}z_{36}-z_{56}r_{36}]}$$

$$\frac{\partial N_4}{\partial r}=\frac{-z_{21}[r_{23}[z-z_3]-z_{22}[r-r_2]]-z_{23}[r_{31}[z-z_1]-z_{31}[r-r_4]]}{[r_{31}z_{41}-z_{31}r_{41}][r_{23}z_{43}-z_{23}r_{43}]}$$

$$\frac{\partial N_4}{\partial z}=\frac{-r_{21}[r_{23}[z-z_2]-z_{23}[r-r_2]]+r_{23}[r_{21}[z-z_1]-z_{31}[r-r_1]]}{[r_{21}z_{41}-z_{21}r_{41}][r_{23}z_{43}-z_{23}r_{43}]}$$

$$\frac{\partial N_5}{\partial r}=\frac{-z_{31}[r_{21}[z-z_1]-z_{21}[r-r_1]]-z_{21}[r_{31}[z-z_1]-z_{31}[r-r_1]]}{[r_{21}z_{51}-z_{21}r_{51}][r_{21}z_{51}-z_{21}r_{43}]}$$

$$\frac{\partial N_5}{\partial z}=\frac{-r_{51}[r_{21}[z-z_1]-z_{21}[r-r_1]]+r_{21}[r_{21}[z-z_1]-z_{31}[r-r_1]]}{[r_{31}z_{51}-z_{31}r_{51}][r_{21}z_{51}-z_{21}r_{51}]}$$

$$\frac{\partial N_6}{\partial r}=\frac{-z_{21}[r_{23}[z-z_3]-z_{23}[r-r_3]]-z_{21}[r_{21}[z-z_1]-z_{31}[r-r_1]]}{[r_{21}z_{61}-z_{21}r_{61}][r_{23}z_{63}-z_{23}r_{63}]}$$

$$\frac{\partial N_6}{\partial z}=\frac{-r_{21}[r_{23}[z-z_3]-z_{23}[r-r_3]]-r_{23}[r_{31}[z-z_1]-z_{31}[r-r_1]]}{[r_{21}z_{61}-z_{21}r_{61}][r_{23}z_{63}-z_{23}r_{63}]}$$